The 70th ICFA Advanced Beam Dynamics Workshop on High Luminosity Circular e+e– Colliders

Improving Beam Quality and Reliability through Low-Level RF Control in Superconducting Accelerators

Feng QIU, Yuan HE, Jinying MA, Lijuan Yang, Tiancai JIANG, Zheng Gao

On behalf of IMP SRF team

Institute of Modern Physics (IMP)

CONTENTS

Introduction（RF ）

- The Radio Frequency (**RF**) systems in particle accelerators are hardware complexes responsible for generating the accelerating fields, including both high-power RF and low-level RF (**LLRF**).

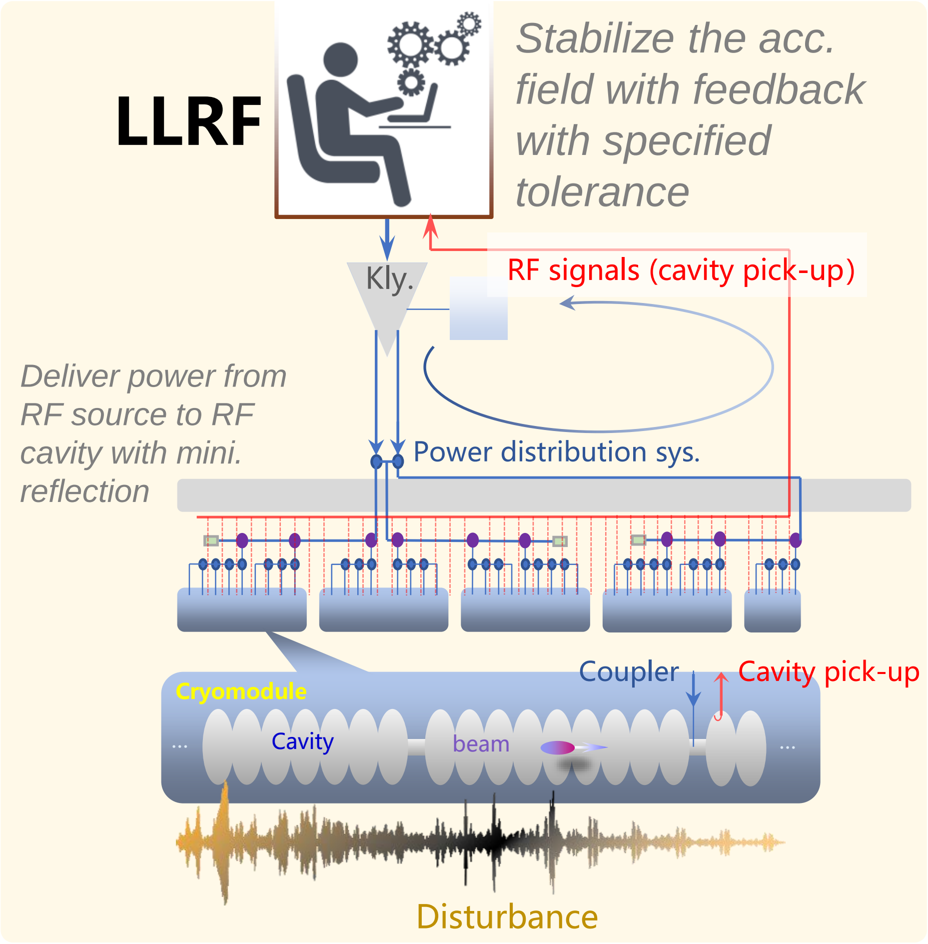

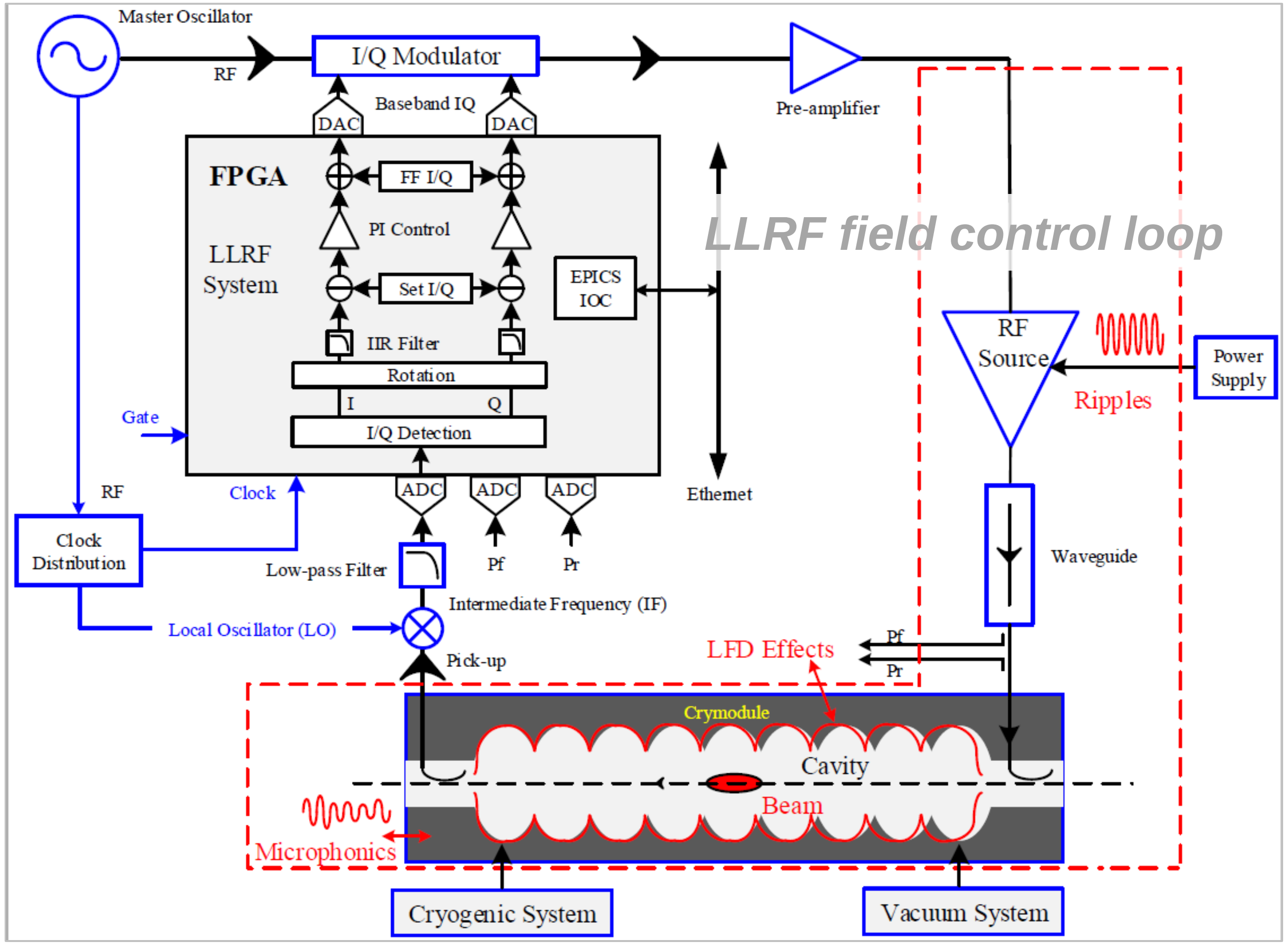

Introduction (LLRF)

- Advanced **LLRF** algorithms are crucial for improving the beam quality

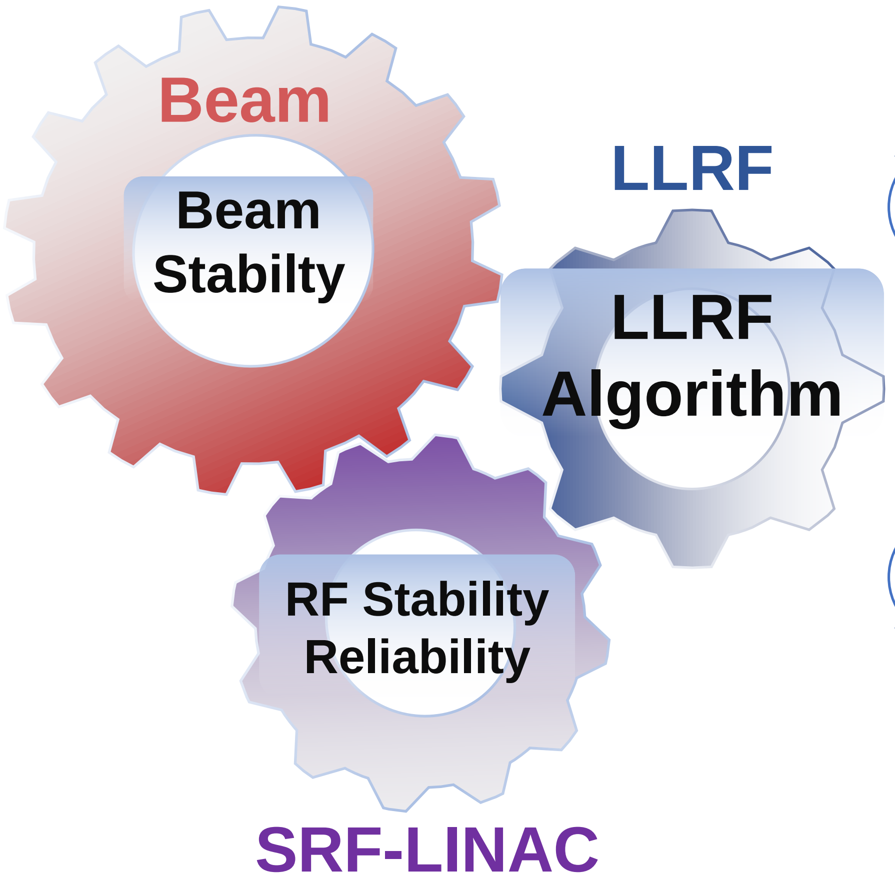

Beam Quality	Enhancing RF stability and reducing beam energy spread	KEK-cERL
Accelerator/Beam Availability	Improving accelerator reliability & beam availability	IMP-CAFe
Automation	AI-based RF fault classification	IMP-CAFe

Introduction (facilities)

- KEK compact Energy Recovery Linac (cERL) & Chinese ADS Front-end (CAFe)

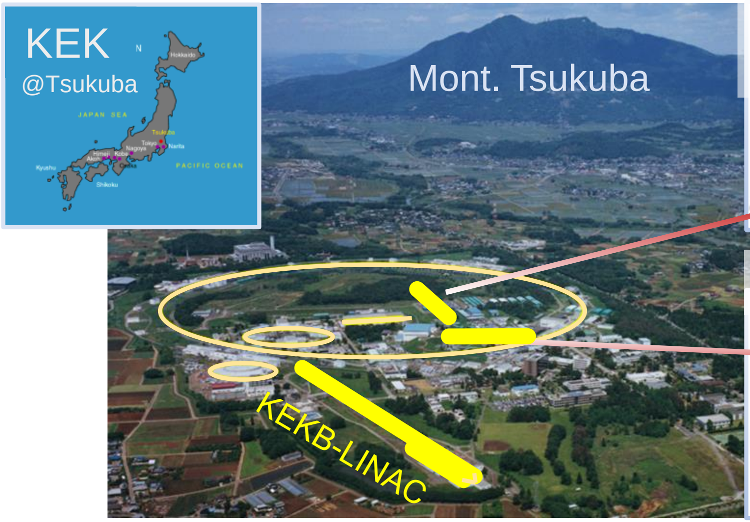

STF (Superconducting test-facility)

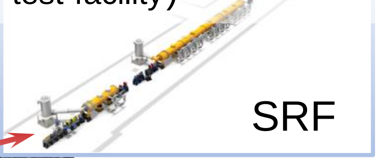

cERL (compact ERL)

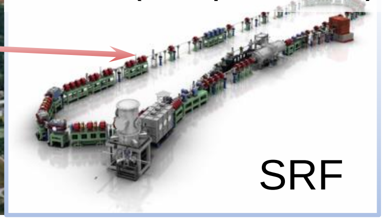

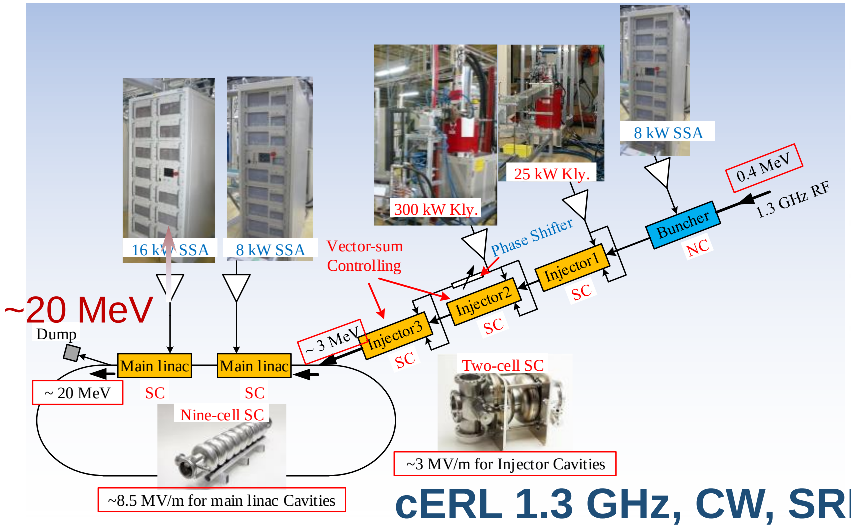

Cav	Q_L	RF Source
Bun	1.1e5	8 kW SSA
Inj_1	1.2e6	25 kW Kly.
Inj_2	5.8e5	300 kW Kly.
Inj_3	4.8e5	
ML_1	1.3e7	8 kW SSA
ML_2	1.0e7	16 kW SSA

cERL 1.3 GHz, CW, SRF

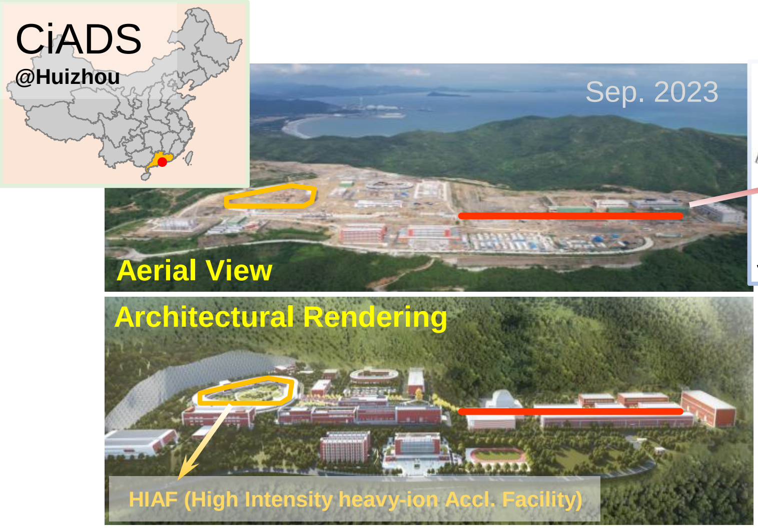

CiADS

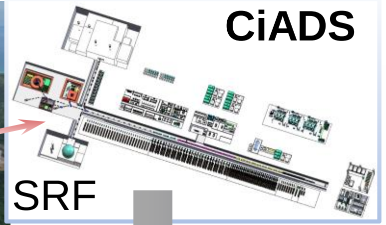

Linac Prototype

- ~20 MeV
- 1 RFQ+ 23 SC
- Q_L: 5e5~1e6
- 10 kW SSA

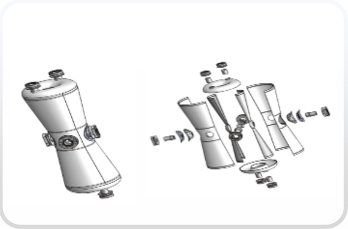

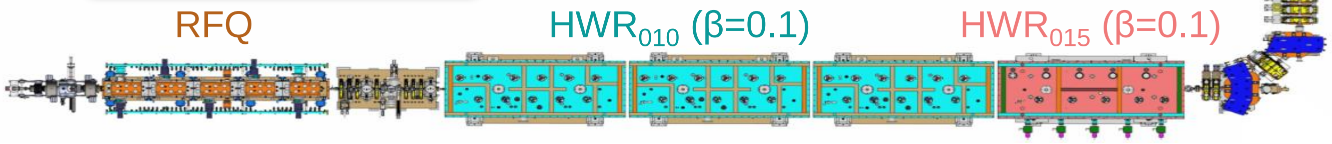

CAFe (Chinese ADS Front-end), 162.5 MHz, CW, SRF

CONTENTS

Pulse Mode Operation @ cERL

- The cERL was once operated in pulse mode to increase beam energy for isotope production
- We observed poor pulse-to-pulse stability under PI control, although intra-pulse stability was satisfactory. Fluctuations in the measured beam energy were noted

Pulse shape

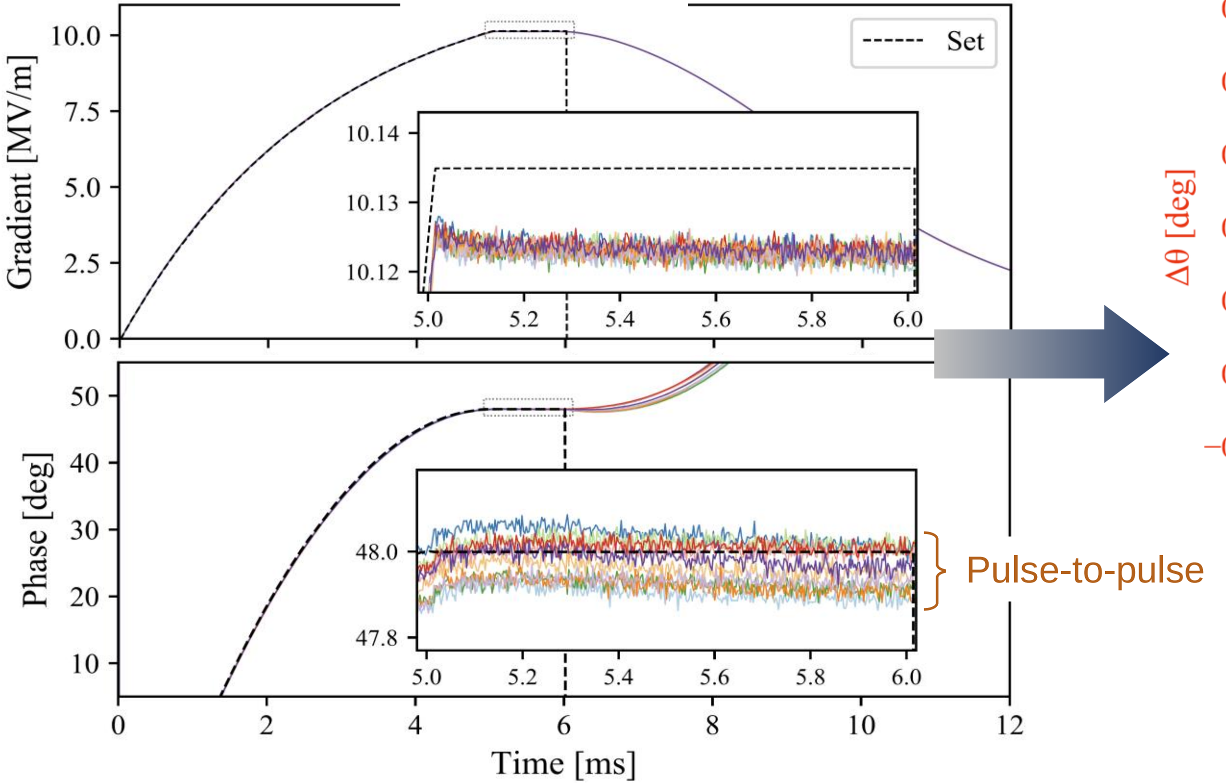

RF Stability (Pulse-to-pulse)

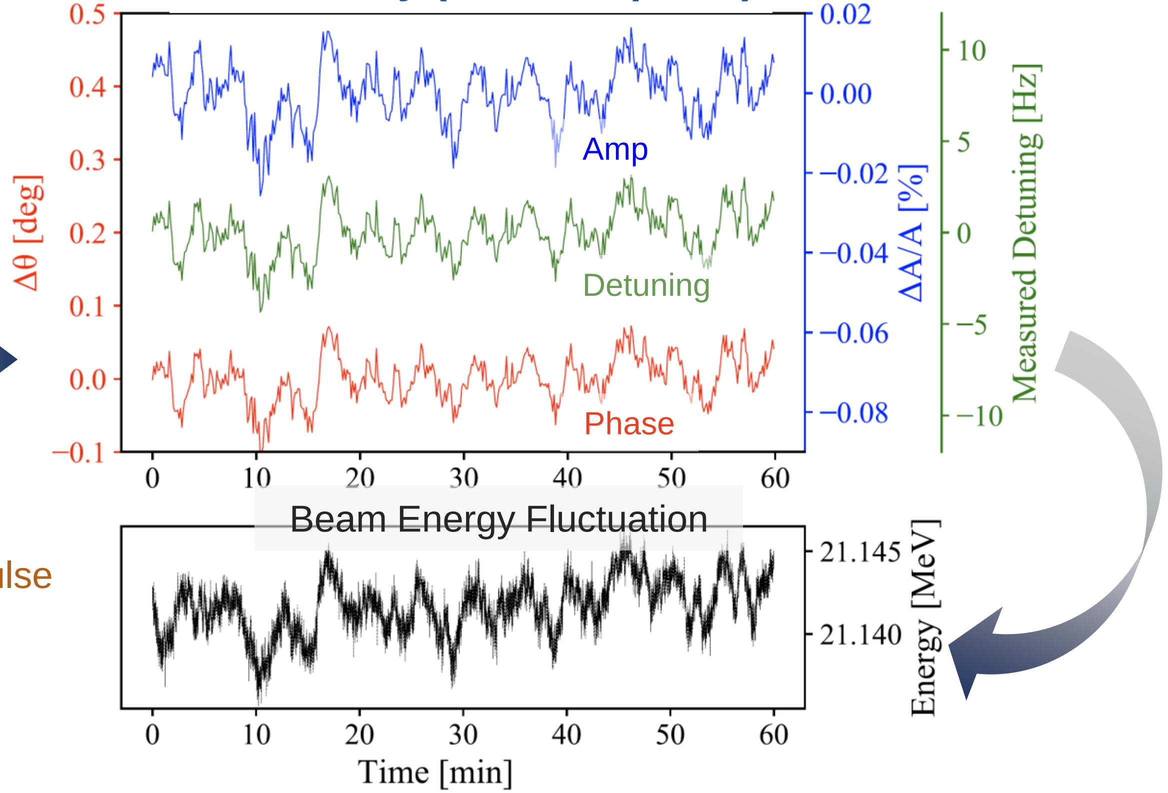

Disturbance Observer-based (DOB) Control

- Disturbance Observer (DOB) ctrl.: Reconstruct **disturbance estimation** ($\hat{d}$), then cancel d with $\hat{d}$ from the LLRF control loop

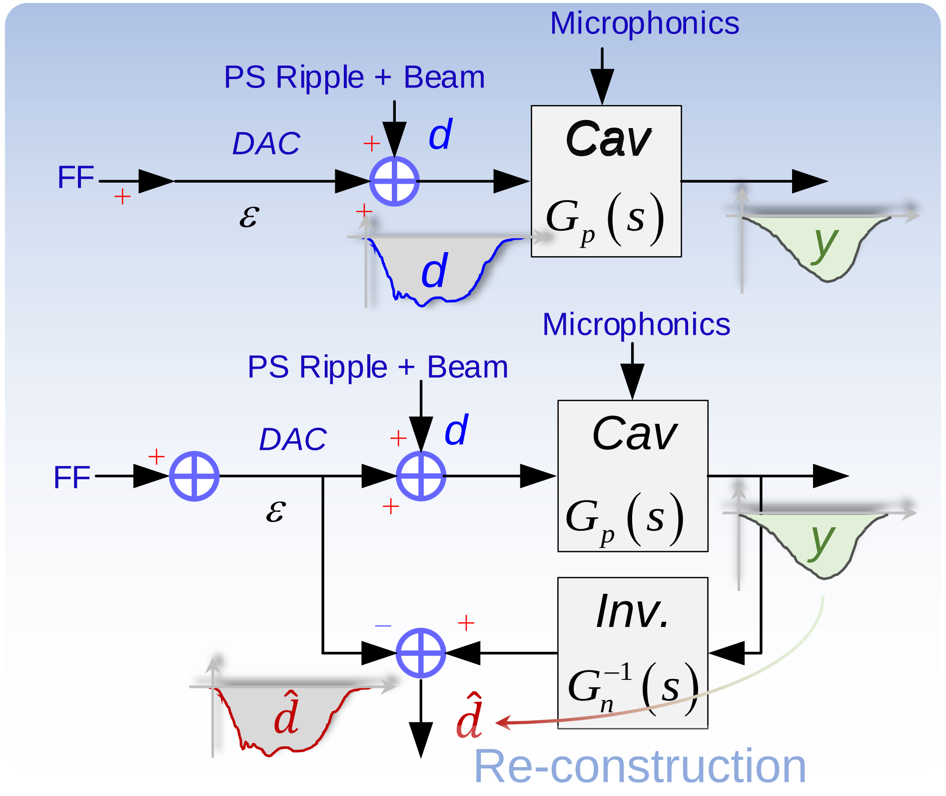

$$\hat{d} = (\varepsilon + d)G_p(s) \cdot G_n^{-1}(s) - \varepsilon = d$$

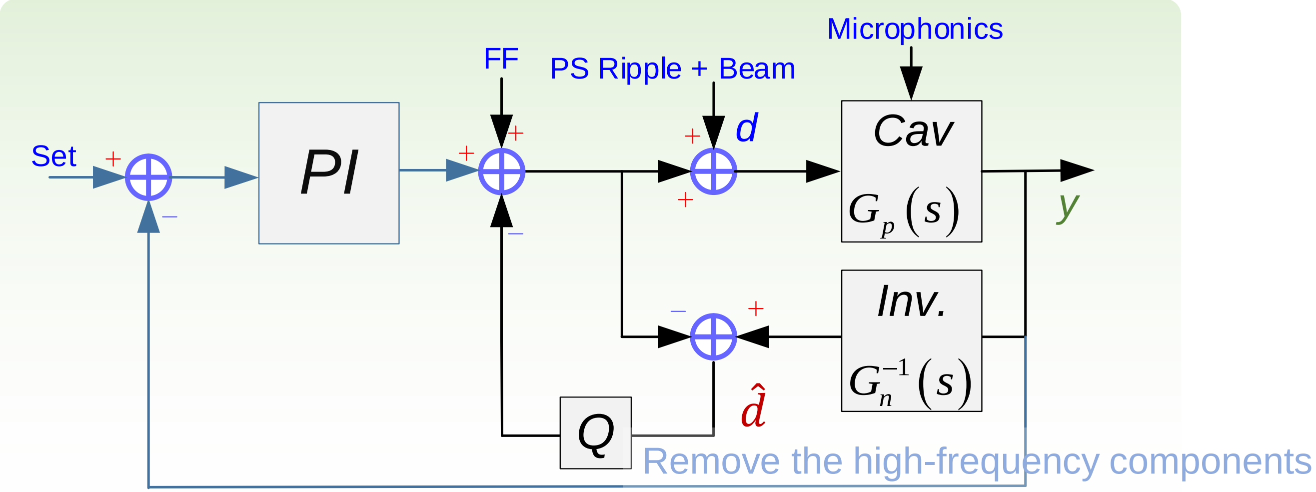

- $H_{PI,d\to y}(s) = \dfrac{G_p(s)}{1 + PI(s)G_p(s)}$
- $H_{PI+DOB,d\to y}(s) \approx [1 - Q(s)] \cdot \dfrac{G_p(s)}{1 + PI(s)G_p(s)}$

$s = j\omega \to 0, Q(s) \approx 1, \to\ 1 - Q(s) \approx 0$

DOB Control (cont'd)

- This control method has been shown to significantly enhance both pulse-to-pulse RF stability and beam energy stability

RF stabilities (intra-pulse)

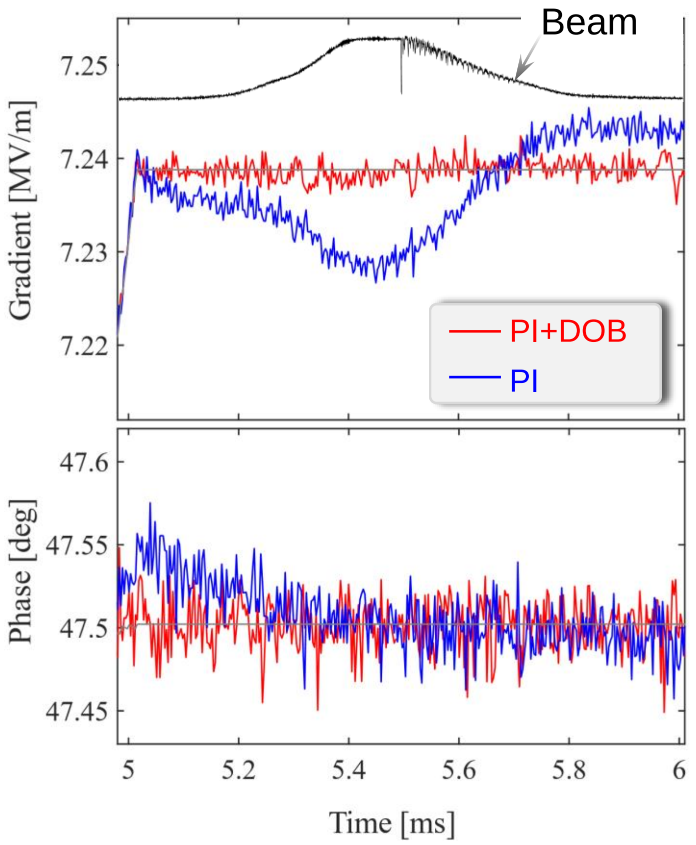

RF stabilities (Pulse-to-pulse)

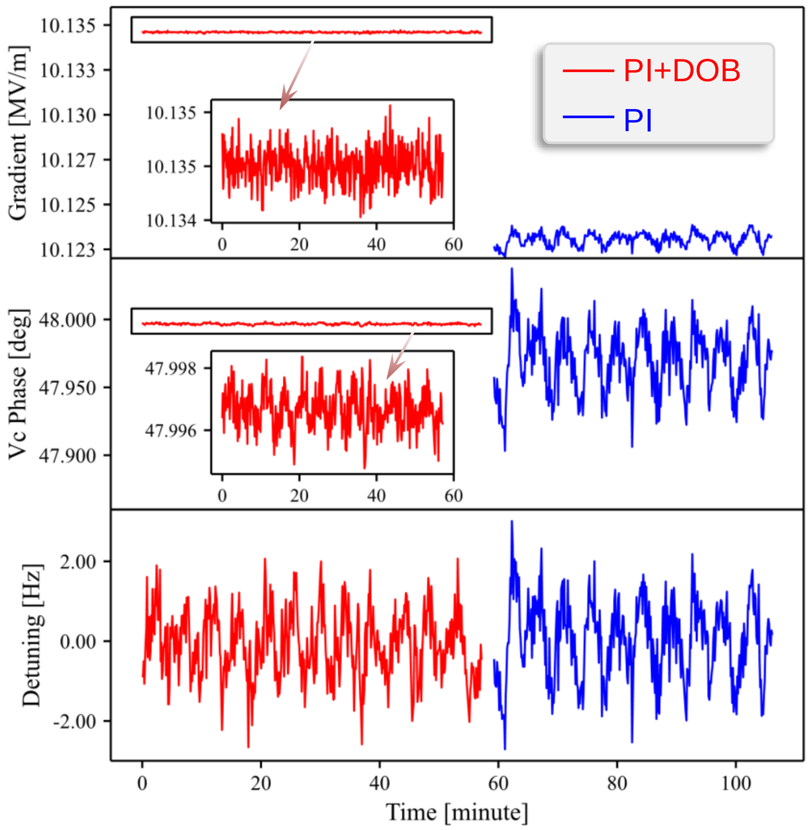

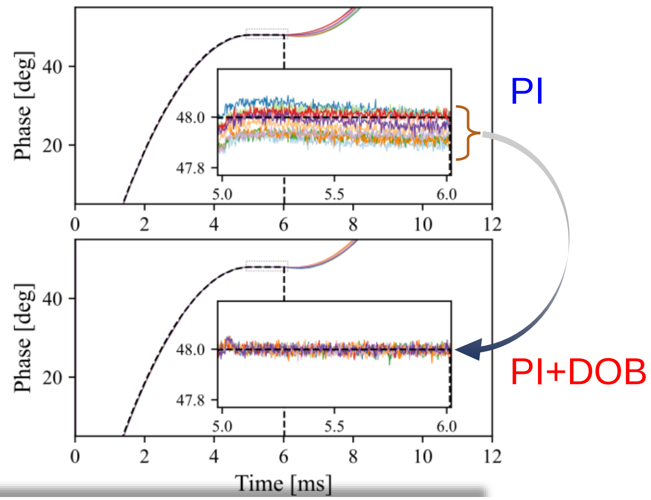

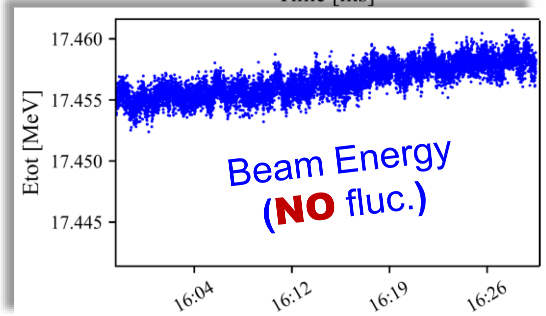

F. Qiu*, et al., Application of disturbance observer-based control on pulsed superconducting radio frequency cavities Phy. Rev. Accel Beam 21, 032003 (2021)

CONTENTS

Transient Loading of 10 mA Beam @ CAFe

- **CAFe** → Stable operation of **10 mA** proton beam
  - In March 2021， CAFe achieved stable operation at hundreds of kW for 100 hours, confirming the feasibility 10 mA beam operation.

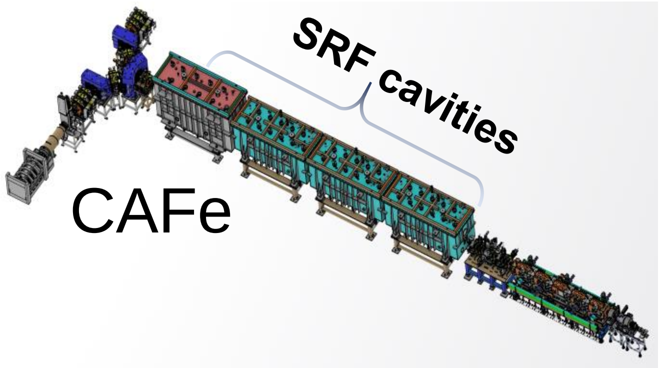

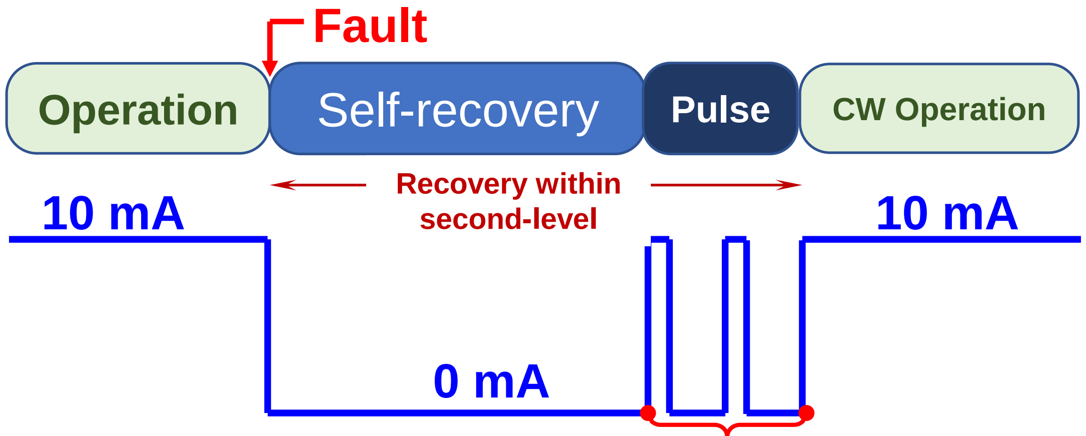

- **CERN-COURIER** evaluates this achievement as an outstanding accomplishment and a **milestone breakthrough** in the field of ADS

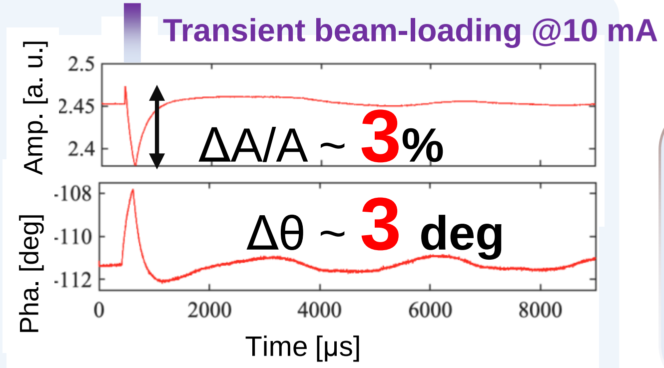

The **transient loading** of a **10 mA** beam is the critical challenge!!

Iterative Learning Control (ILC)

- **Iterative Learning Control** (ILC) →widely used for beam-loading compensation
  - Step1: Calibrate the error between the reference signal (*r*) and cavity pick-up signal (*y*)

$$e_j(k)=r_j(k)-y_j(k)$$

  - Step2: Update the current feedforward (FF) output (u_{j+1}) using the previous FF (u_j) and error (e_j)

A matrix or a zero-phase filter

$$u_{j+1}(k)=\mathbf{Q_{ILC}}[u_j+\mathbf{L}(e_j)]$$

A matrix or a plant-inversion-model or PID

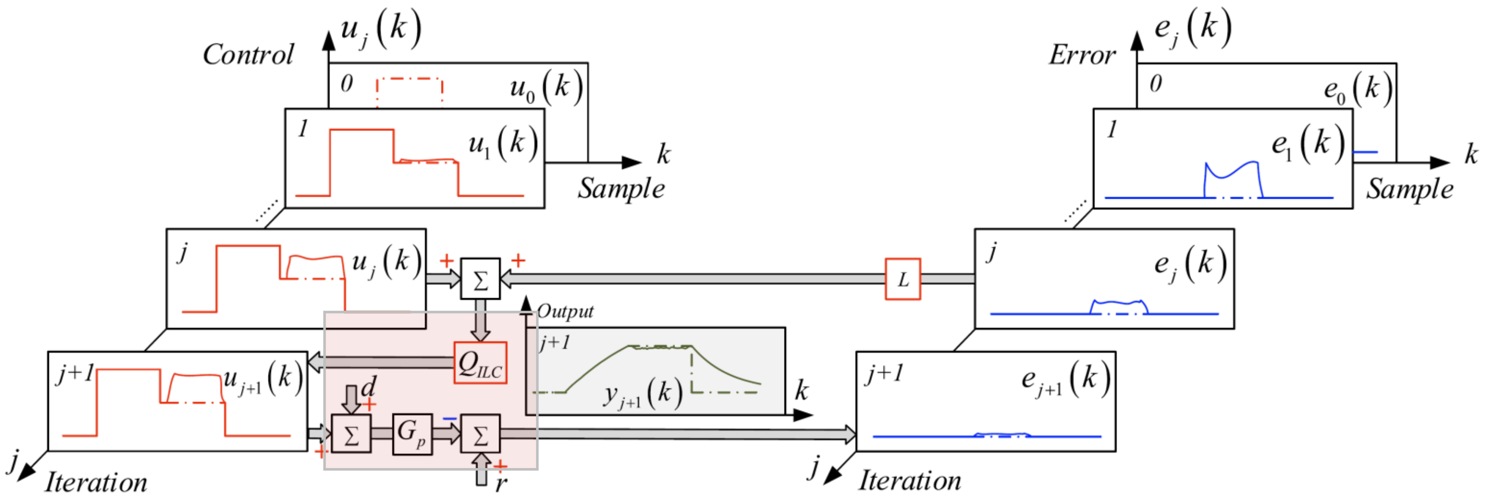

The main ILC algorithm is usually implemented outside FPGA

E.g. Norm Optimal ILC

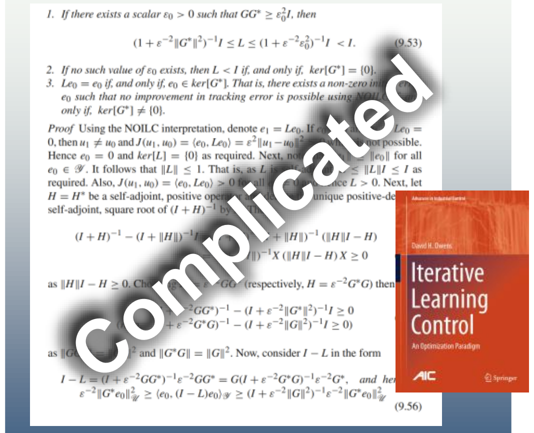

—— D. H. Owens, Springer, 2015

FPGA-based ILC (Basic Idea)

- In most cases, a beam pulse can be considered **quasi-rectangular**, which means the FF could also be rectangular pulse. This assumption may significantly simplify the algorithm design

Beam profile @ CAFe

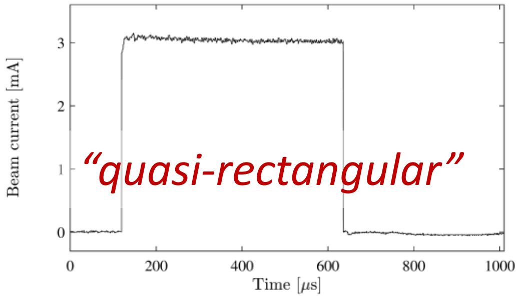

$$u_{j+1}(k) = \mathbf{Q}_{\mathbf{ILC}}[u_j + \mathbf{L}(e_j)]$$

$$\begin{cases} u_{j+1}(k) = \varepsilon_j + F_j, \ \varepsilon_j = L(e_j) \\ F_{j+1} = F_j + E_j \end{cases}$$

Constant Value (only a register inside FPGA)

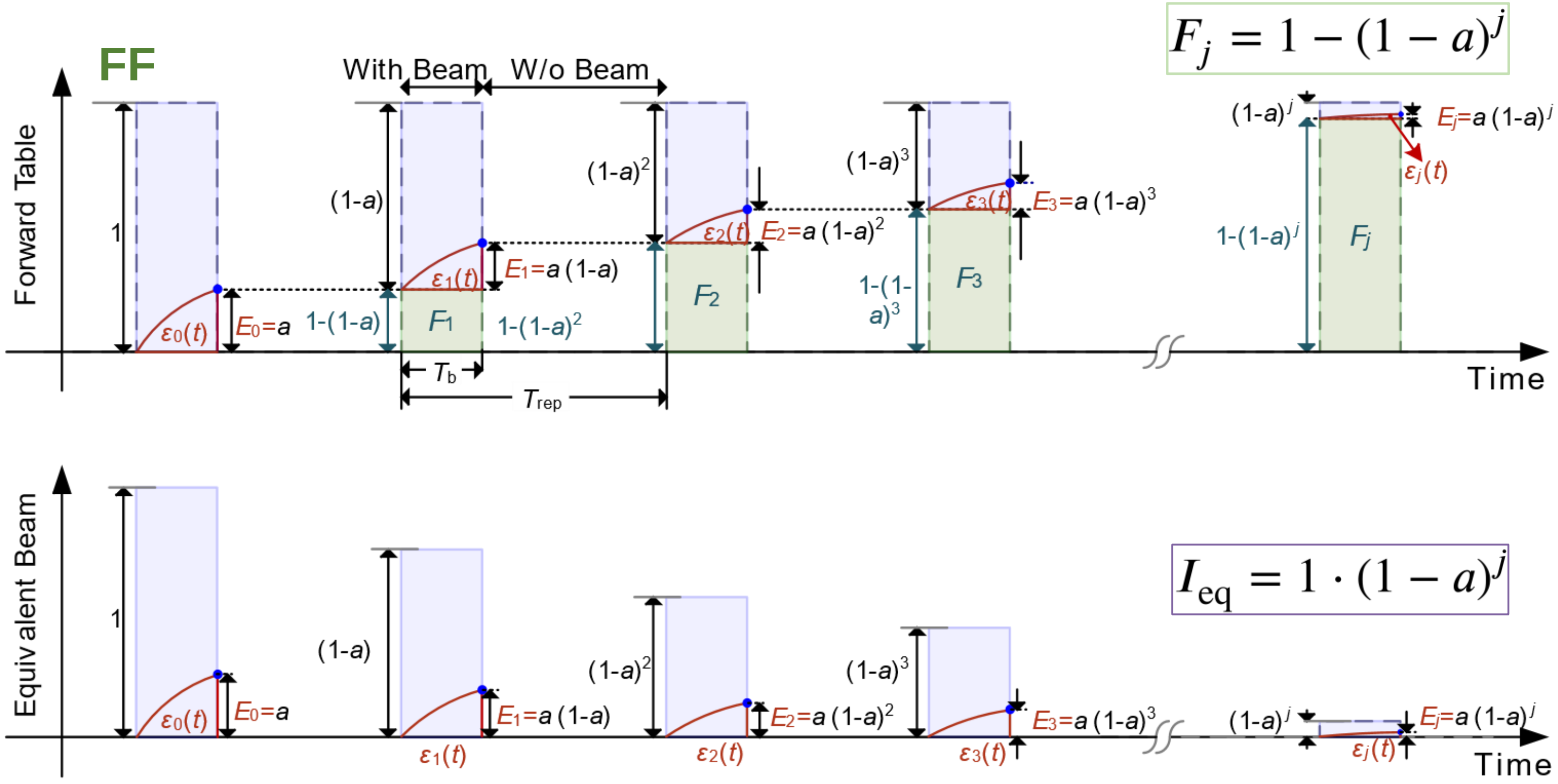

FPGA-based ILC (Confirmation)

- The new ILC algorithm was demonstrated during the CAFe beam-commissioning
  - **High band-width:** works in 1 MHz repetitive rate;

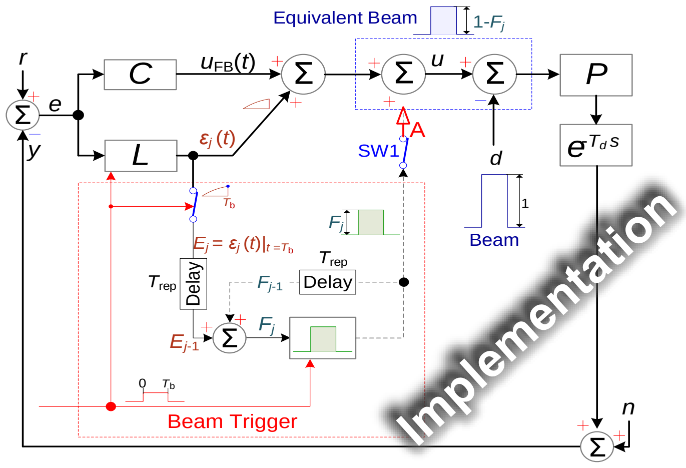

Field Amp. Field Pha.

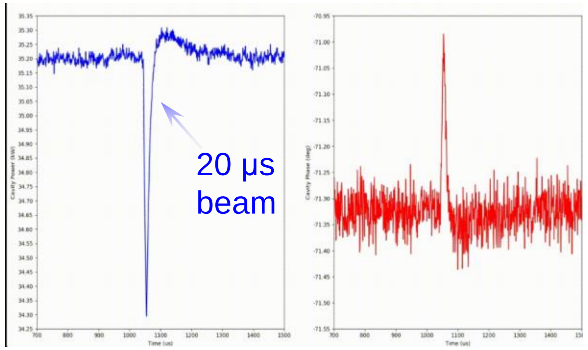

RF waveforms during iter. proc.

Cav. Field FF

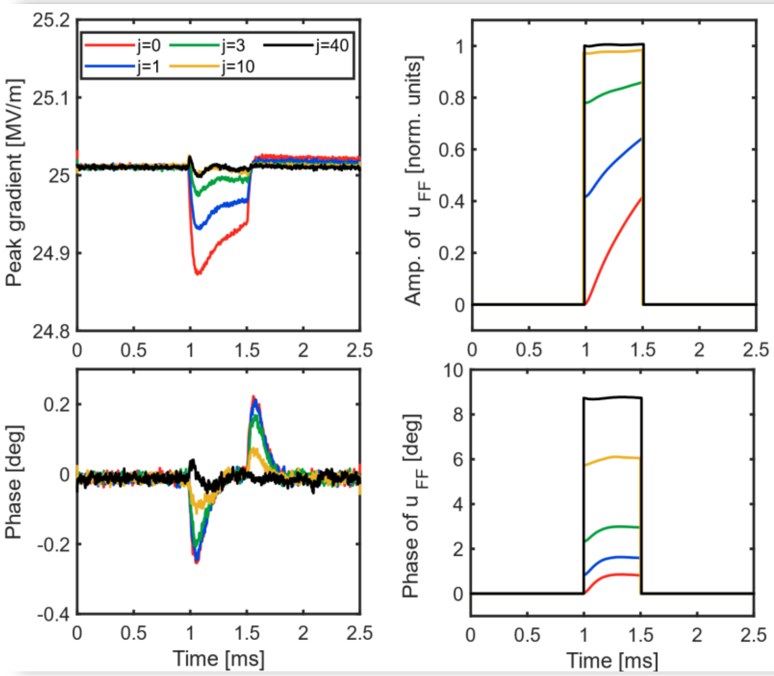

Convergence curve

Cav. Field FF

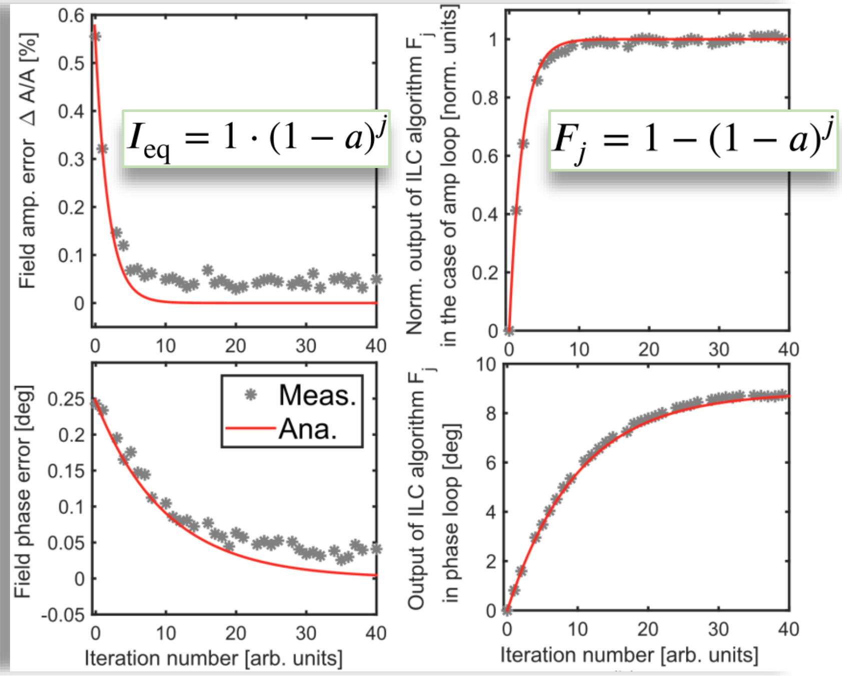

C. Y. Xu, et al., Application of a modified iterative learning control algorithm for superconducting radio-frequency cavities, Nucl. Instrum. Methods. A . 955,166237 (2022)

CONTENTS

SRF faults at CAFe

- Two typical SRF faults that were confused CAFe for a long time
  - Field emission (FE)-induced **burst-noise** appears in the cavity pick-up signal
  - **Pondermotive instabilities** typically indicates the non-linear coupling btw the electrical and mechanical modes

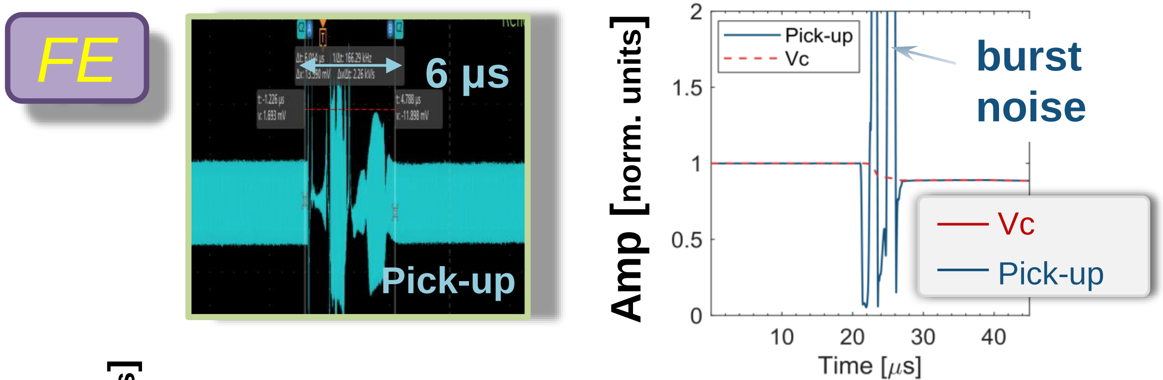

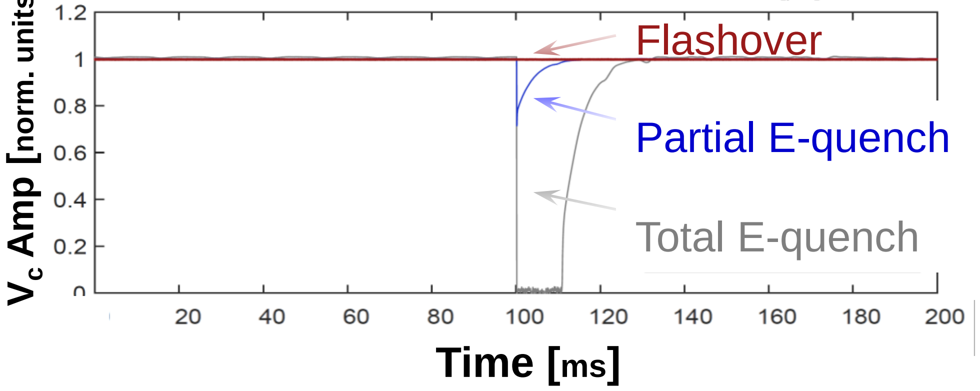

*The burst noise can lead to **an unexpected LLRF response,** resulting in a cavity fault*

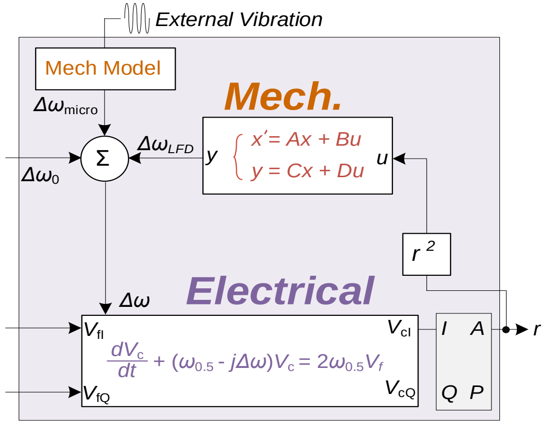

Transfer function of Mech. mode

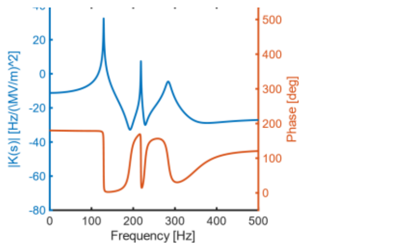

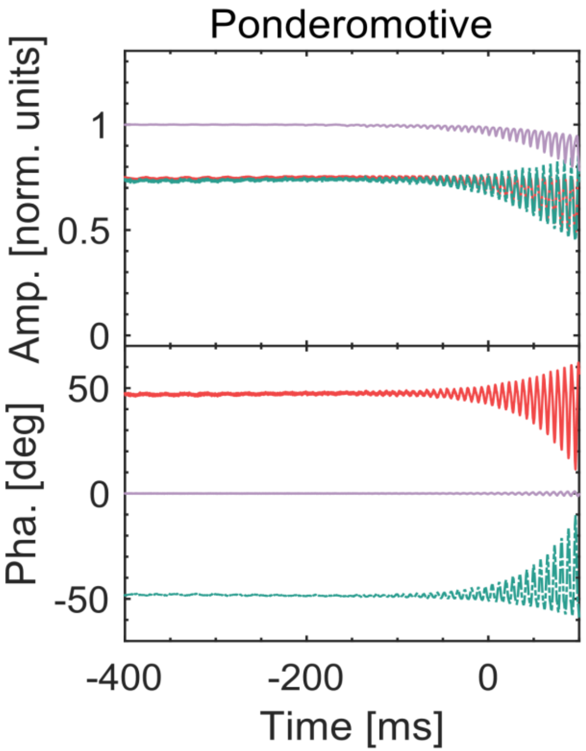

The accelerating gradient and detuning beginning to oscillate with increasing amplitude

Mitigation of Burst-noise-induced SRF Faults

- When the LLRF system detects a burst-noise event, it immediately generates a burst-noise trigger, which remains active for a time interval of ΔT (>15 μs, longer than the burst noise period)
- During the burst-noise period, PI output (u_{PI}) is **overwritten by u_{delay}** which holds the data from u_{PI} **0.8 μs prior** to burst-noise trigger; then the u_{PI} is maintained until the trigger is over

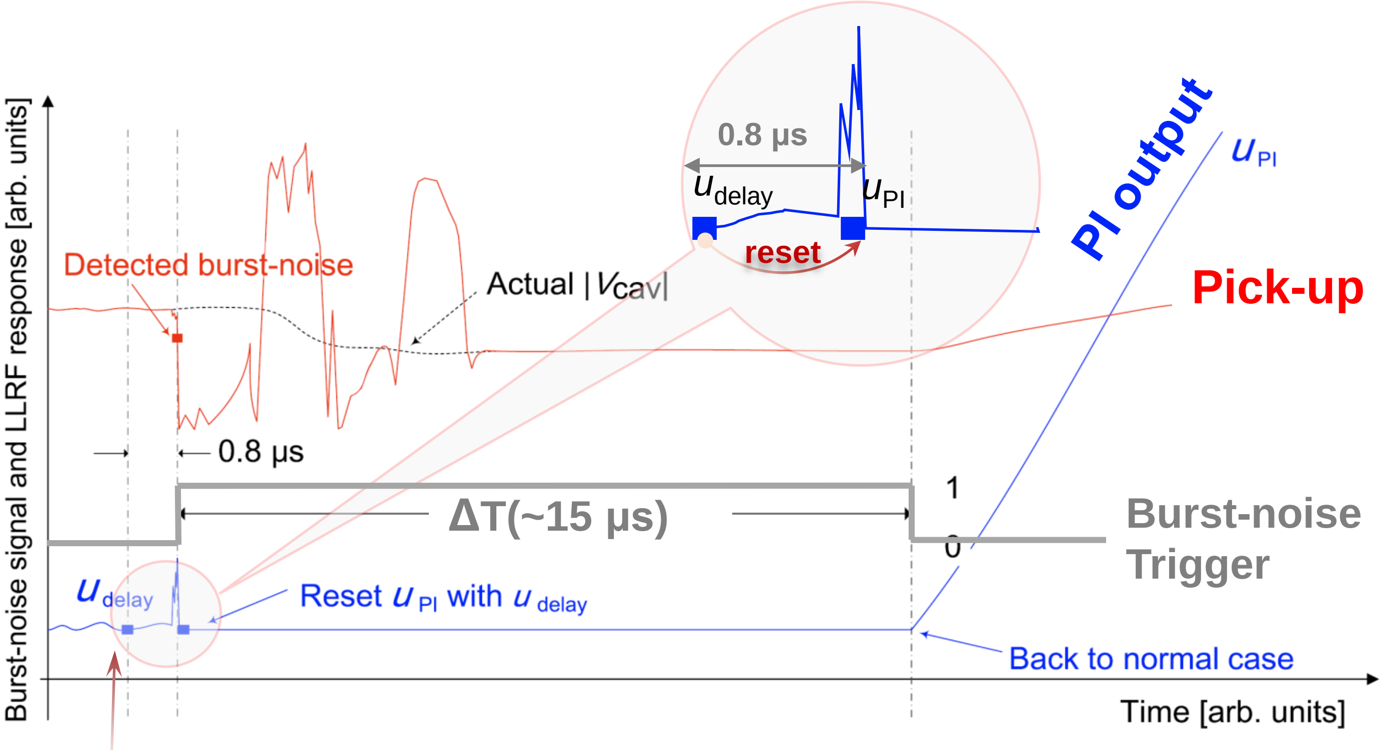

u_{delay} is the PI output during the normal state operation

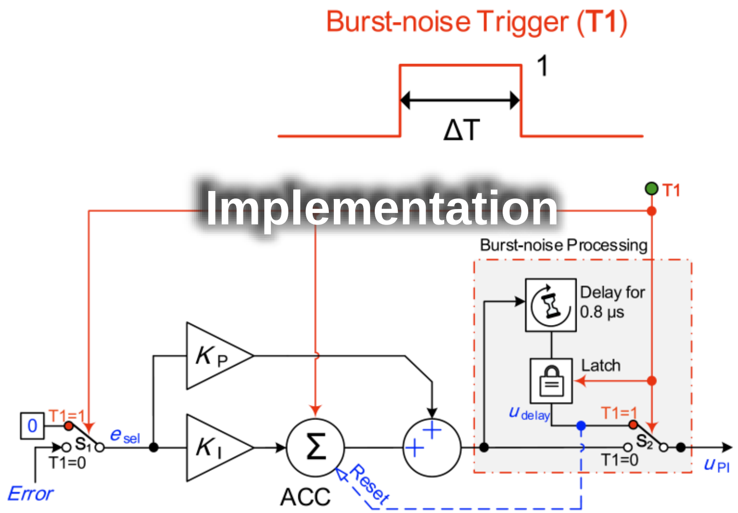

Mitigation of Burst-noise-induced SRF Faults

- The unexpected LLRF response can be eliminated
- The effectiveness of the proposed algorithm was confirmed during the long-term operation

Cavity pick-up

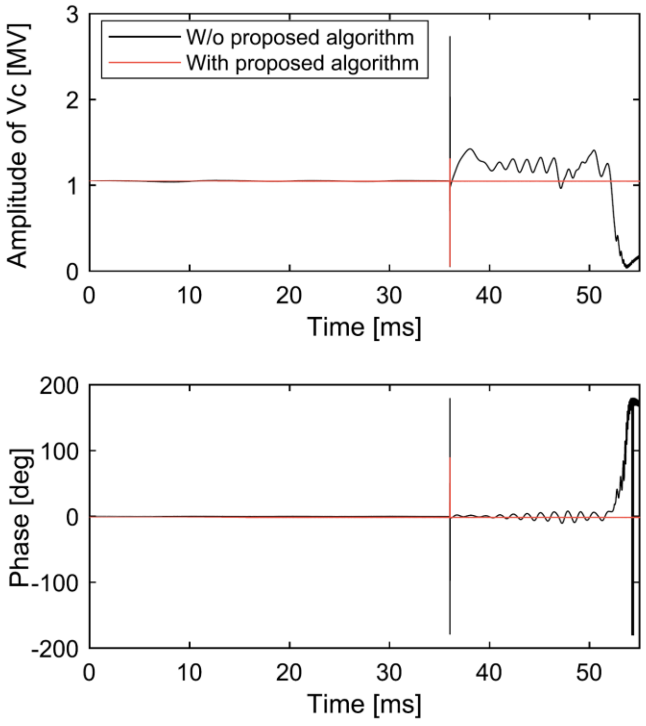

Cavity forward

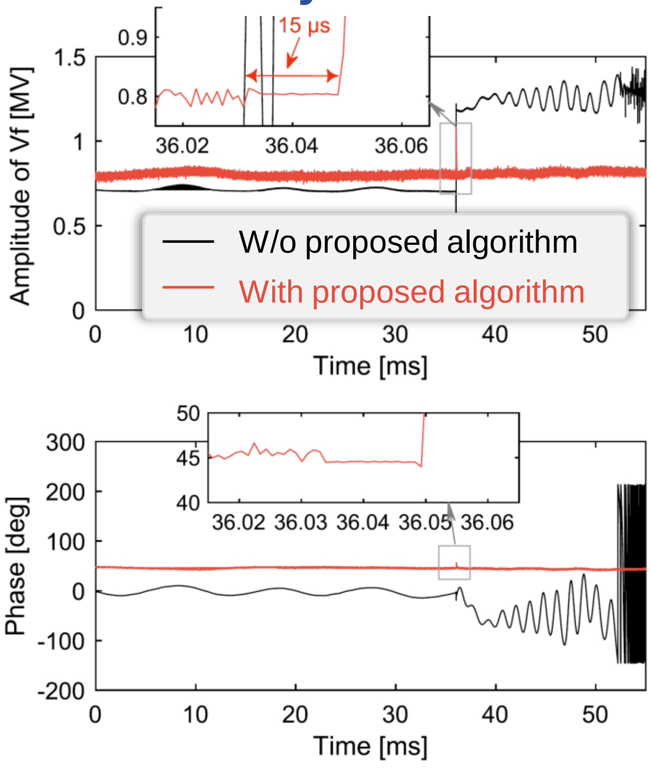

Beam

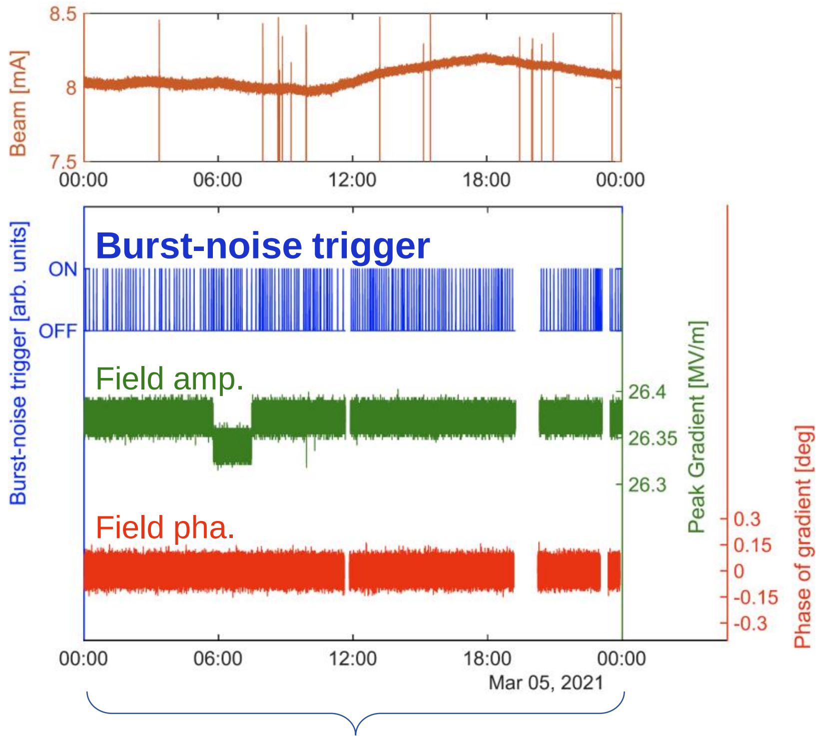

24 hours

Mitigation of Ponderomotive Instabilities

- Proper feedback control may shrink the unstable region

W/O LLRF FB

With LLRF FB

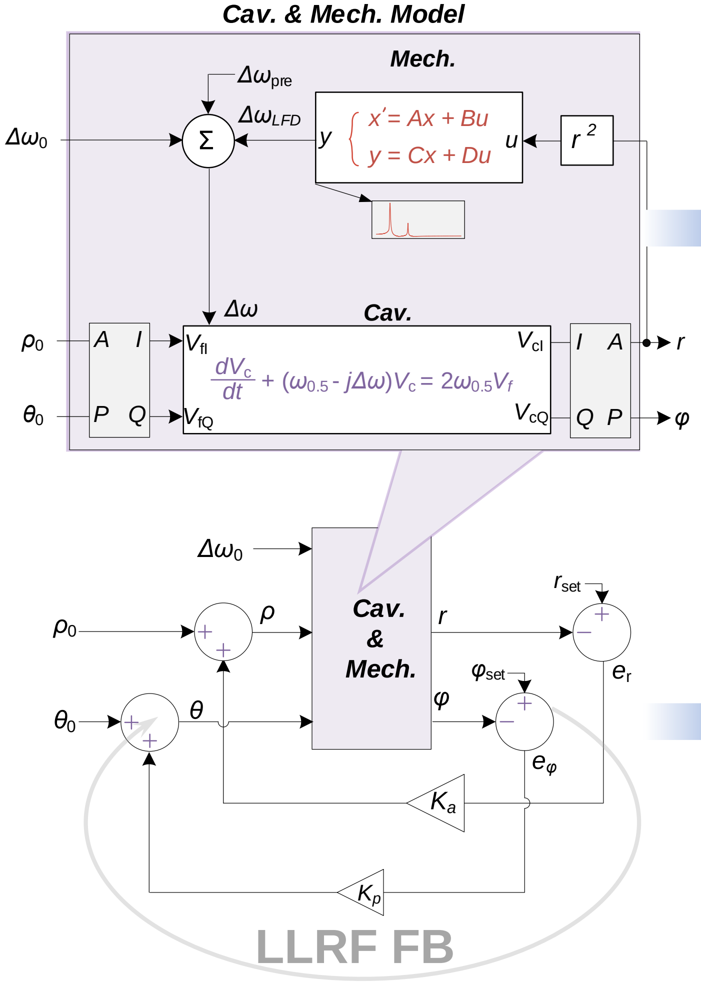

System Matrix (Open loop)

$$A_{OL} = \begin{vmatrix} s+\omega_{1/2} & \Delta\omega & 0 & 0 \\ -\Delta\omega & s+\omega_{1/2} & -\omega_{1/2} & 0 \\ 0 & 0 & 1 & \frac{2G\cdot b\cdot\omega_m}{\omega_{1/2}} \\ \frac{1}{s^2+bs+\omega_m^2} & 0 & 0 & 1 \end{vmatrix}$$

Cav

Mech.

$$|I-\lambda A_{OL}|<=0$$

λ: eigenvalue

System Matrix (Closed loop)

$$A_{FB} = \begin{vmatrix} s+\omega_{1/2} & \Delta\omega & -\omega_{1/2} & -\Delta\omega & 0 & 0 \\ -\Delta\omega & s+\omega_{1/2} & \Delta\omega & -\omega_{1/2} & -\omega_{1/2} & 0 \\ K_a & 0 & 1 & 0 & 0 & 0 \\ 0 & K_p & 0 & 1 & 0 & 0 \\ 0 & 0 & 0 & 0 & 1 & \frac{2\cdot G\cdot b\cdot\omega_m}{\omega_{1/2}} \\ \frac{1}{s^2+bs+\omega_m^2} & 0 & 0 & 0 & 0 & 1 \end{vmatrix}$$

FB

$$|I-\lambda A_{FB}|=0$$

Unstable boundary

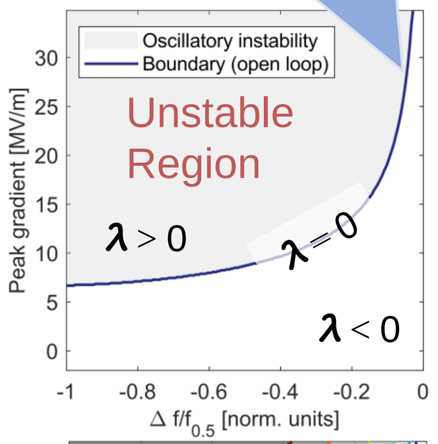

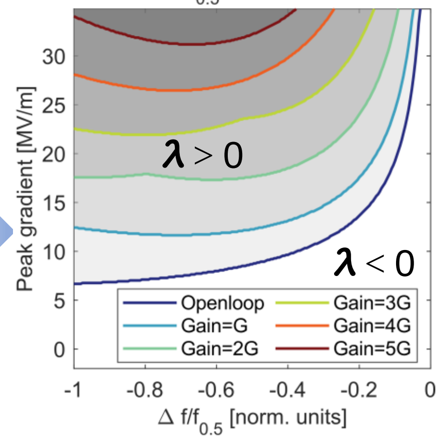

$K_a = K_p =$ Gain

S. K. Koscielniak, Ponderomotive Instability of Generator-Driven Cavity, in Proc. of IPAC 2019, Melbourne, Australia, 2019

Mitigation of Ponderomotive Instabilities

- Ponderomotive instabilities was mitigated by optimizing the LLRF FB parameters

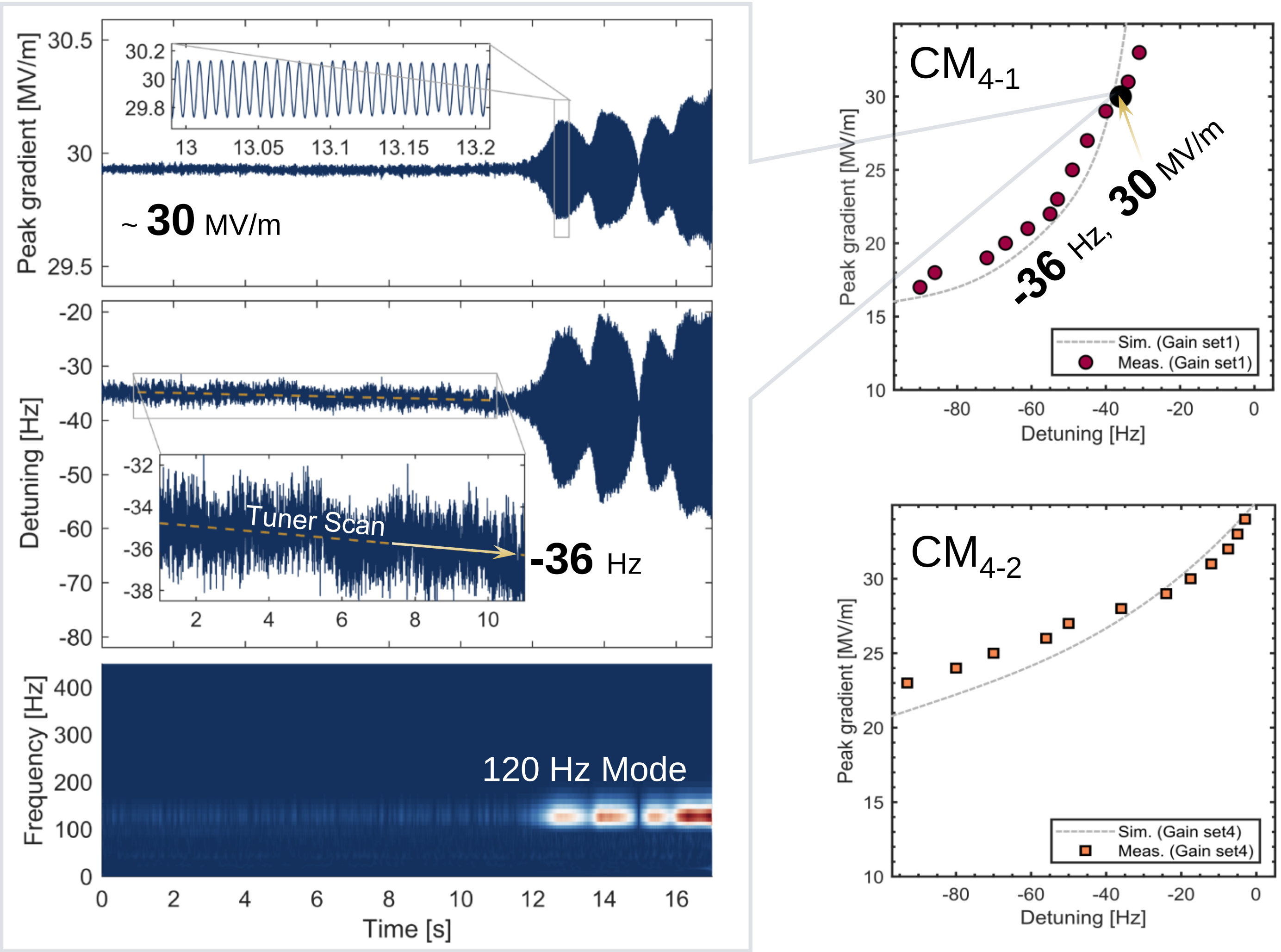

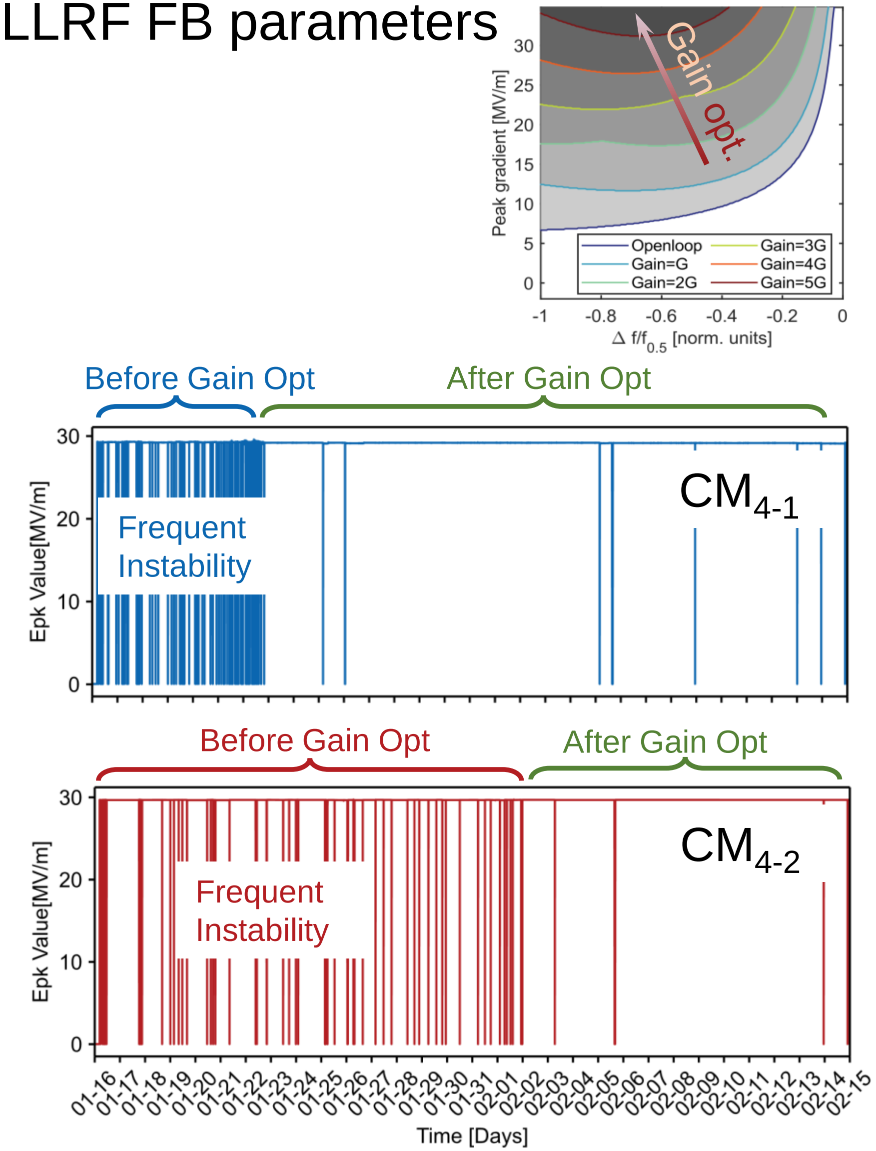

CONTENTS

Classification of SRF Faults

- Collect the critical-waveform data (cavity voltage, forward/reflected…) by digital low-level radio-frequency (LLRF) DAQ systems
- Data-analysis were performed by subject matter experts

Cavity voltage (V_c), forward (V_f*)/reflected (V_r*) and DAC output (V_{LLRF}) signals are recorded (*10 kHz ~ 100 kHz, 50000 samples for each signal*)

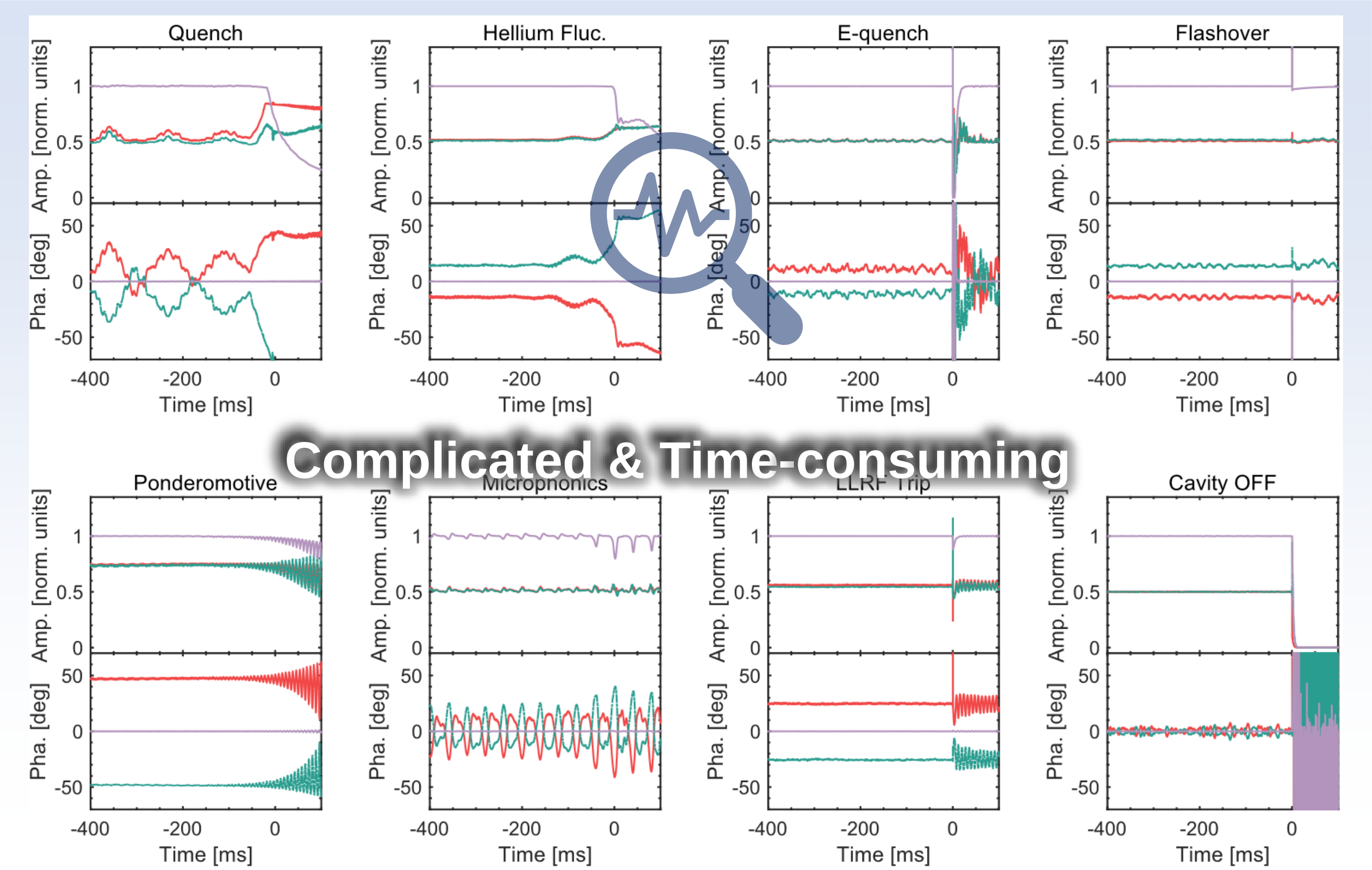

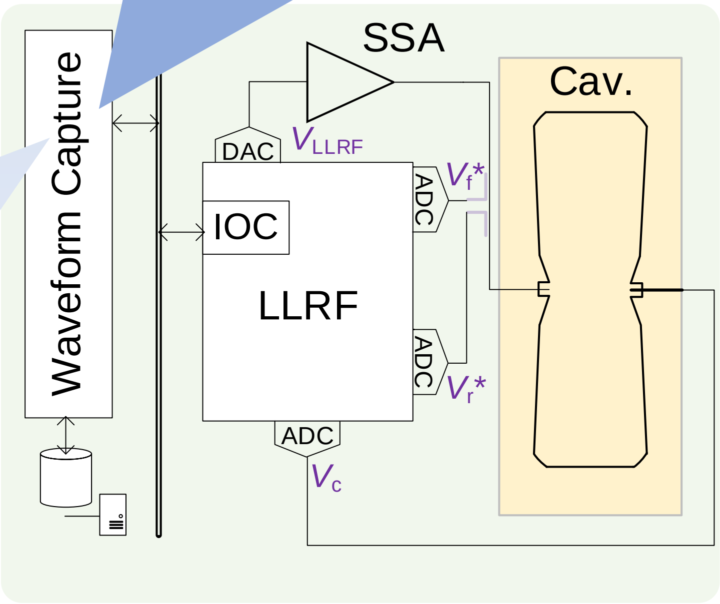

Expert-based fault analysis requires expertise and intuition (*which makes it difficult to provide real-time fault feedback to operators*)

→ Automatically Fault Classification (using ***machine learning tech.***)

C. Tennant et al., Phys. Rev. Accel. Beams, 11 871 (2020) 114601

ML-based SRF Faults Classification

- Eight patterns were recognized and labeled by subject matter experts
- Expert-based feature engineering method were applied

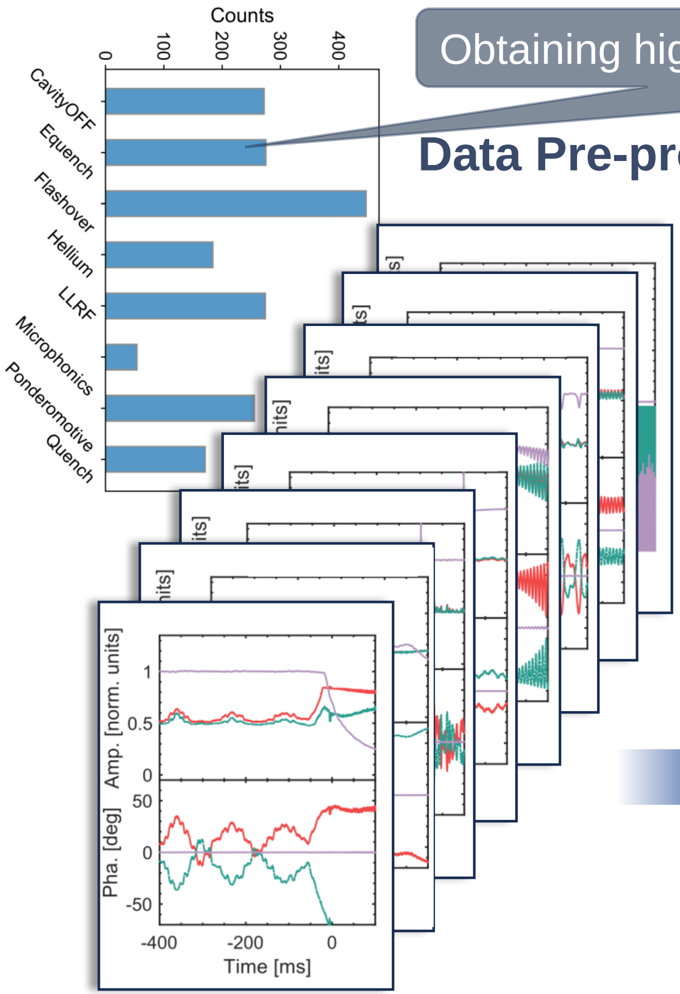

Obtaining high-quality, well-labeled event data is the essential first step

Data Pre-processing **Feature Engineering** **Supervised ML-based SRF faults classification**

JLAB → Autoregression (AR)-based Feature-Extraction

$$X_t = c + \varphi_1 X_{t-1} + \varphi_2 X_{t-2} + \cdots \varphi_p X_{t-p}$$

Require the signal to be autocorrelated, resulting in difficulty in capturing the abrupt fault patterns in CAFe (e.g. , E-quench & flashover)

$\varphi_1, \varphi_2, \cdots \varphi_p$

Weights of AR Model

Expert experience-based Feature-Extraction

What we have applied in this presentation

$Q_{id}, E_{id}, \cdots r_{rms2}$

Eight expert-defined features

Machine Learning

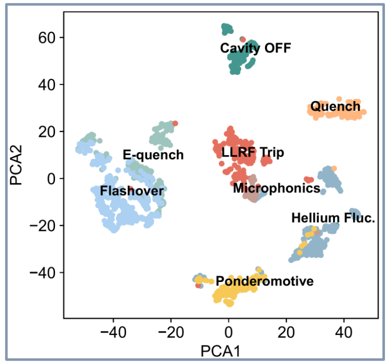

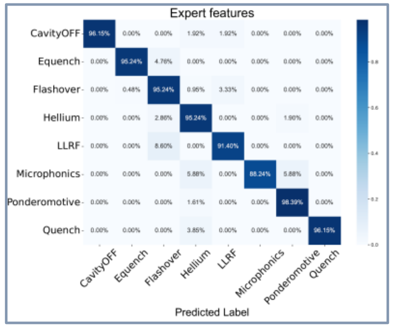

Feature Engineering

- Distribution of expert-defined features

Eight features for each fault events

Features	Q_{id}	F_{max}	F_{ratio}	$\Delta\Theta$	E_{id}	$\Delta\rho_{max}$	r_{rms1}	r_{rms2}
Method	Modeling	Freq. Domain Analysis		Signal Characteristic			Statistical Feature	

Merits

- Limited numbers of features
- Features are physically meaningful
- Features are not affected by the DAQ sampling rate

Drawbacks

- Specific algorithms are required
- Generalizability & Scalability need further validation

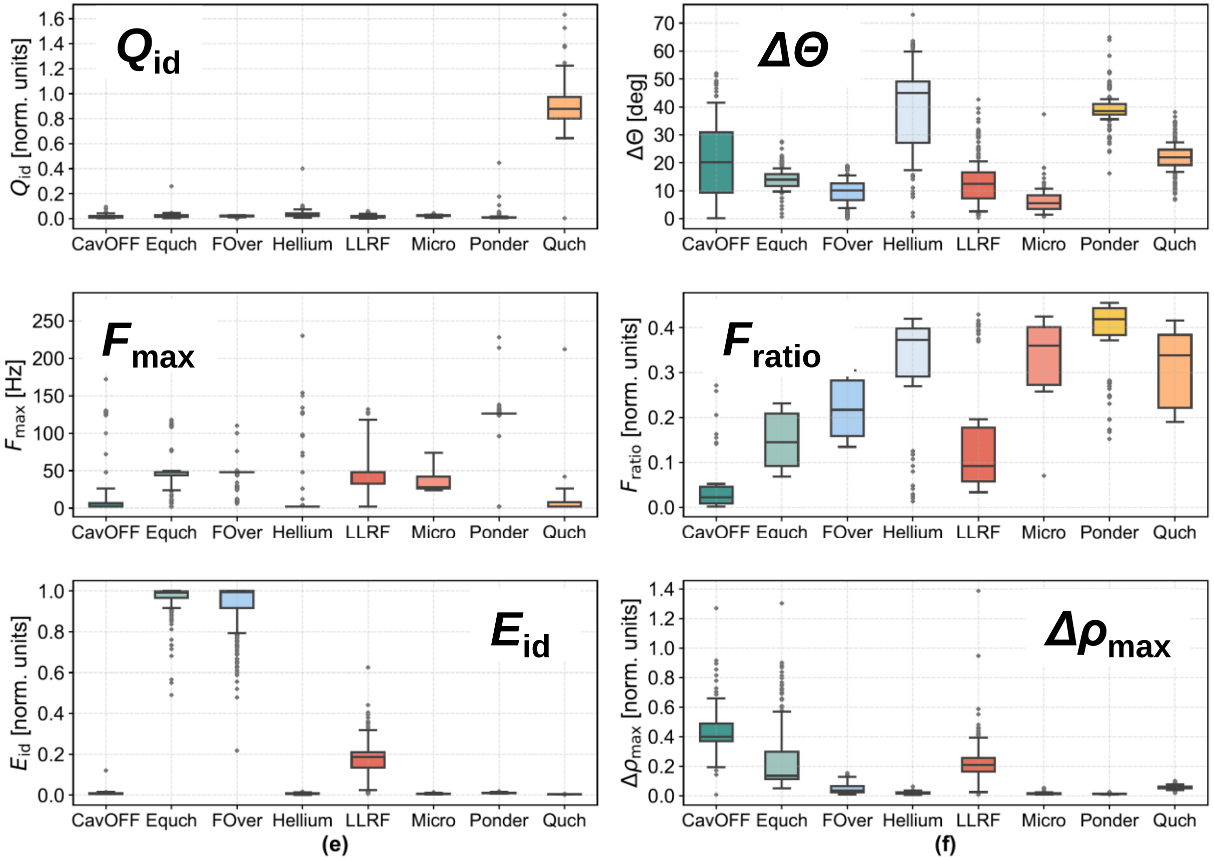

Result of the ML Model

- **Prediction Accuracy: ~94**% (Expert) v.s. ~**89**% (AR)
- **XGB** (eXtreme Gradient Boosting) model wins by a small margin

	SVM (OneVsOne)	XGB	RFs
AR (3)	0.860 ± 0.0108	0.895 ± 0.0129	0.900 ± 0.0101
AR (4)	0.862 ± 0.00980	0.884 ± 0.00711	0.891 ± 0.0115
AR (5)	0.862 ± 0.00970	0.885 ± 0.00729	0.886 ± 0.00829
Expert	0.918 ± 0.0124	0.947 ± 0.0105	0.945 ± 0.00802
AR + Expert	0.949 ± 0.00701	0.959 ± 0.00408	0.959 ± 0.00612

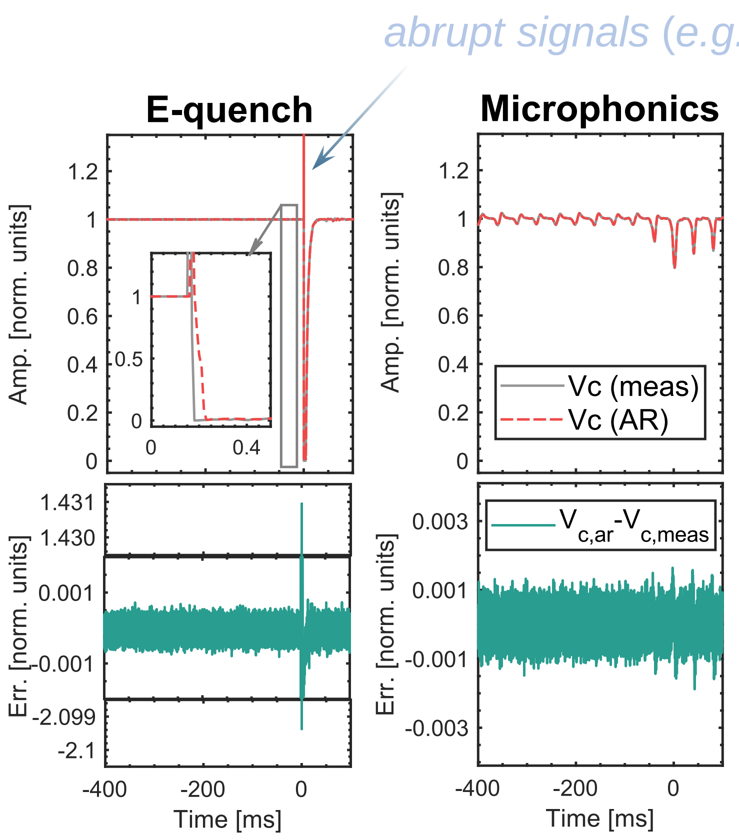

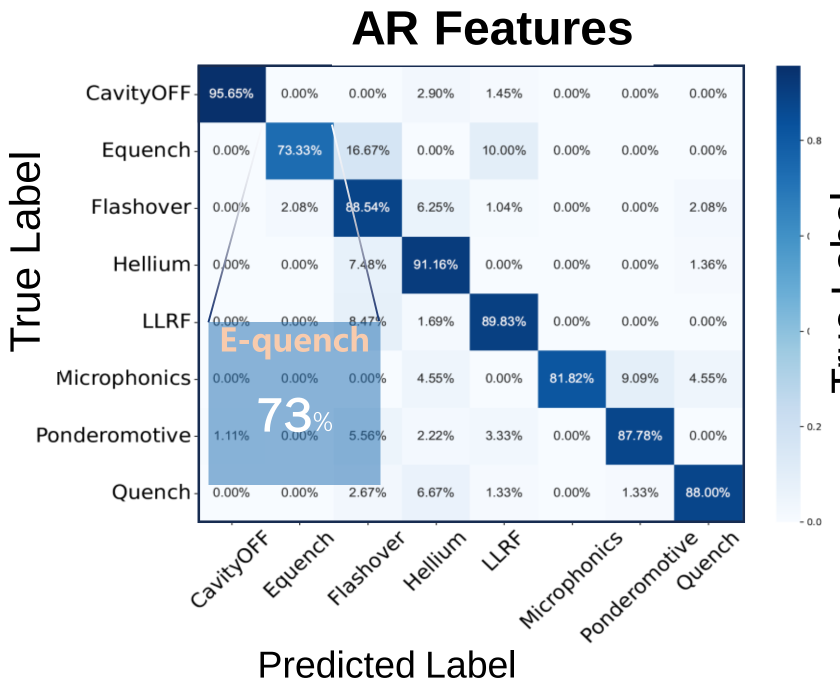

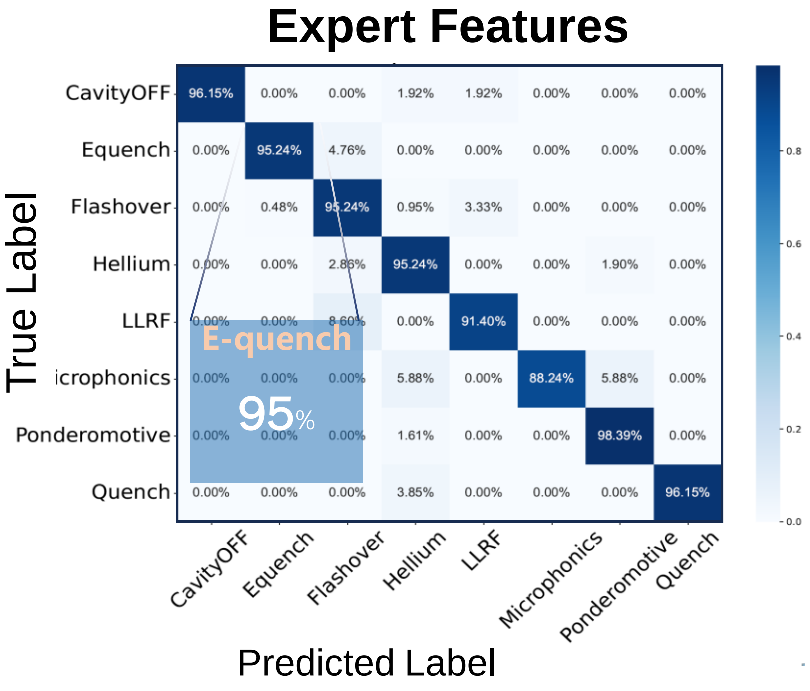

Big Data Analysis

- ML models can automatically classify SRF faults
- Big data analysis helps confirm which cavity suffers from specific fault patterns.

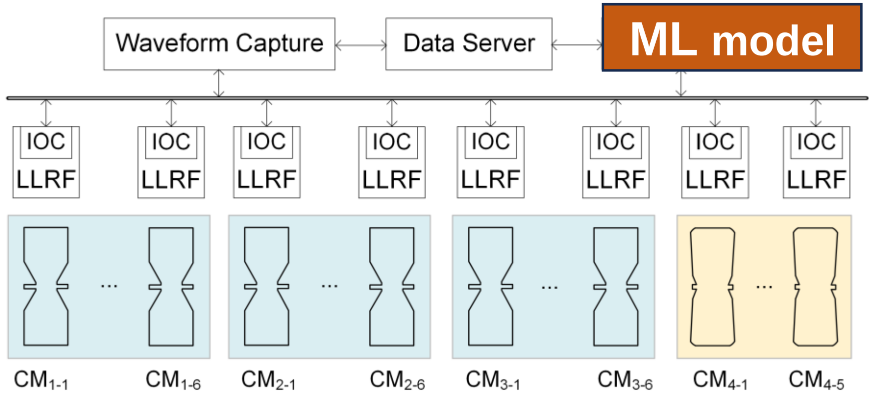

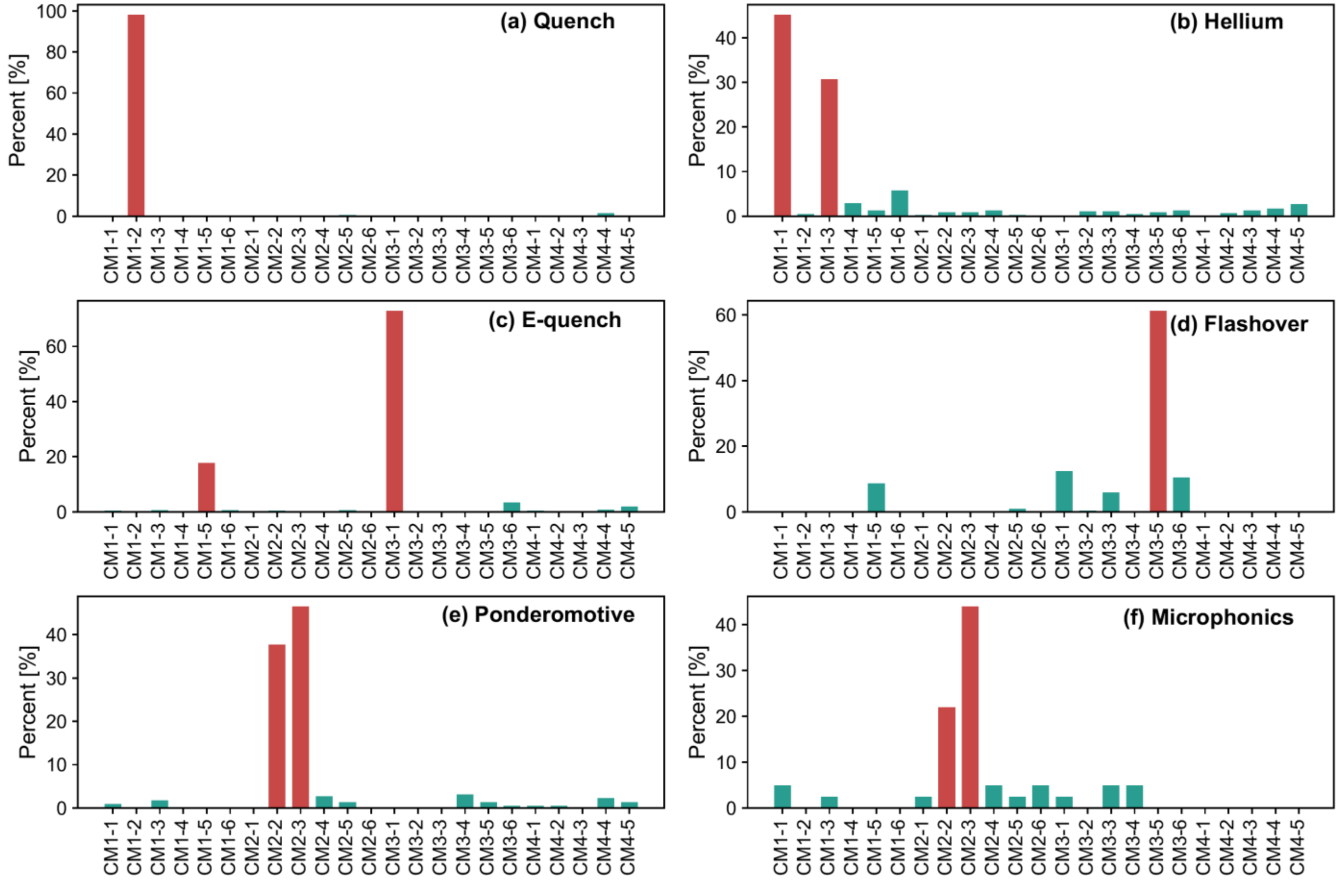

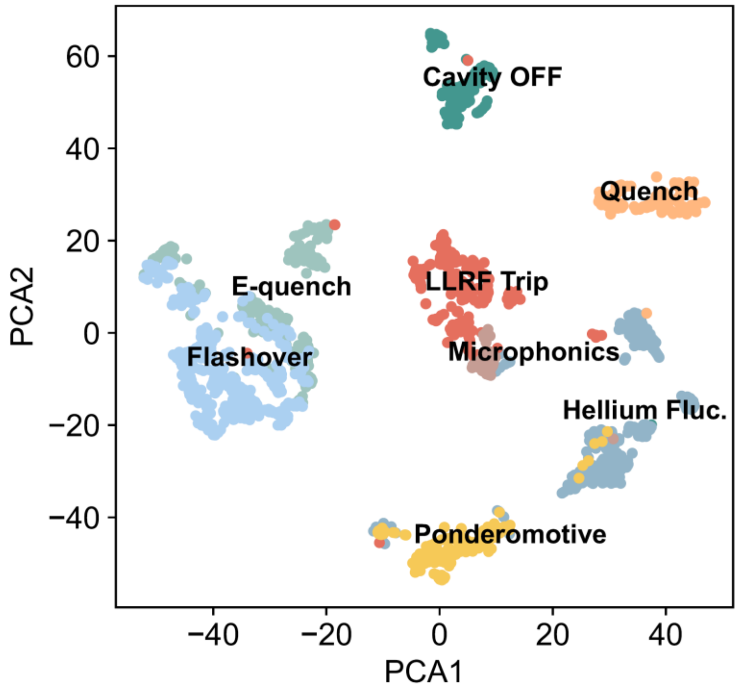

Summary

- Enhancing RF stability and reducing beam energy spread using DOB control strategies
- Managing transient loading of the 10 mA beam with new Iterative Learning Control (ILC) strategies
- Achieving AI-based automated SRF fault classification
- Mitigating SRF faults using flexible LLRF algorithms

Thanks for your attention

Back-up Slides

Subcategorization of Quenching Faults

- **The** ML models suggest that the quench events can further divided into 3 patterns

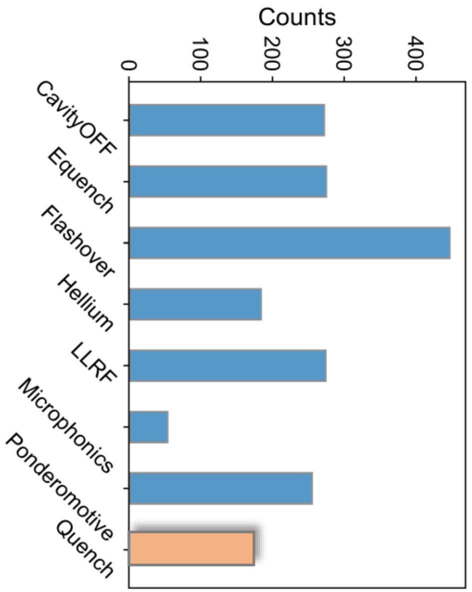

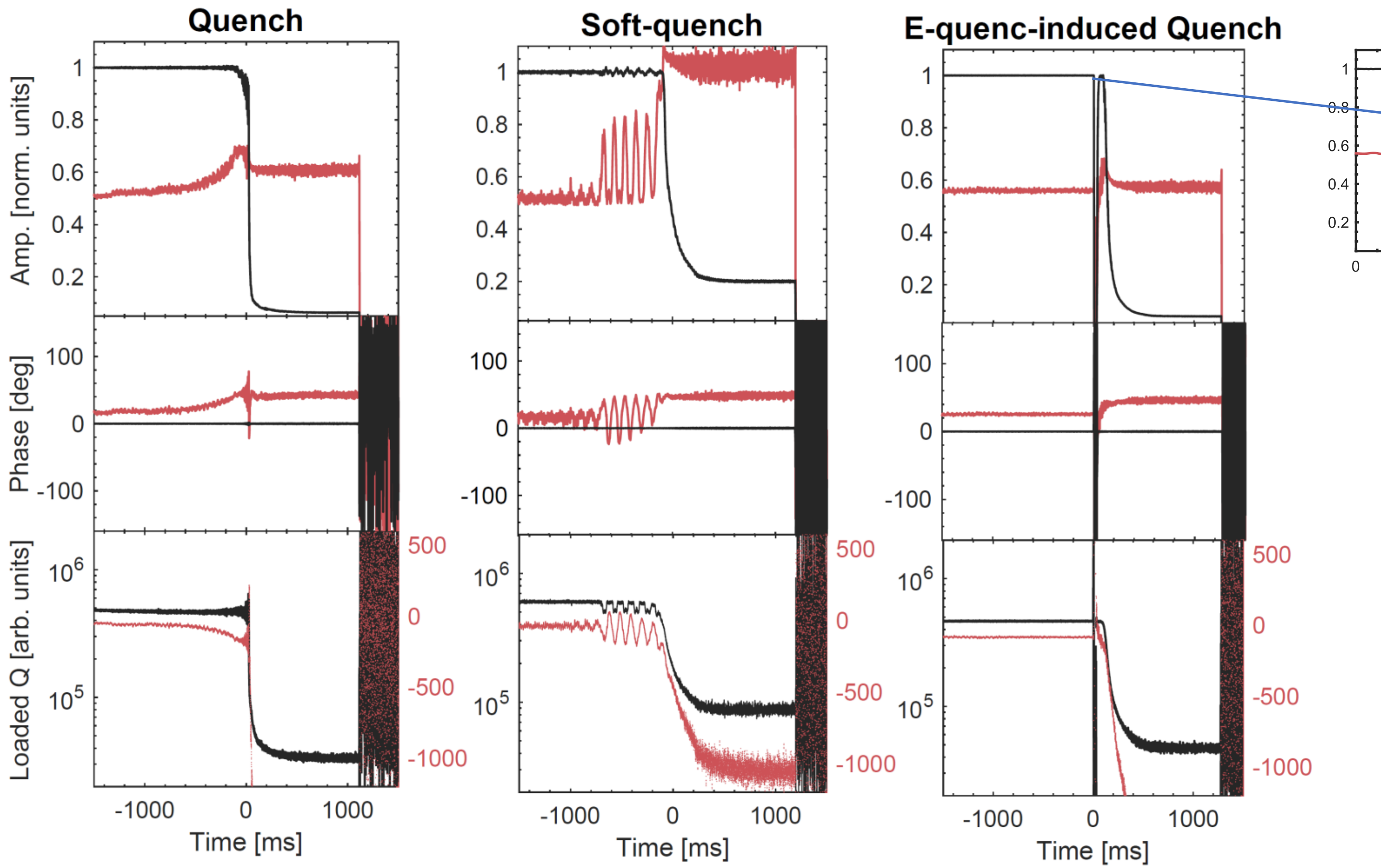

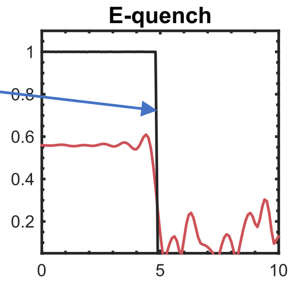

Overall Quench Events

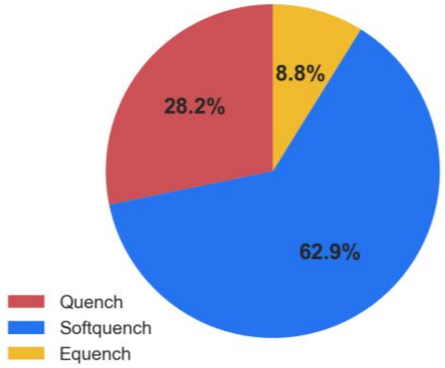

Dark-current Characteristic

- The “partial E-quench” is accompanied by **dark-current** which can be seen as a kind of beam-loading. It is possible to characterize the dark current using the **“beam induced RF transient”**

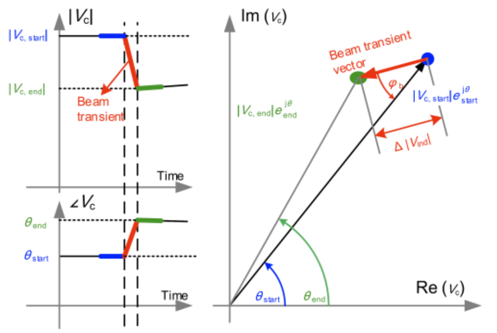

Partial E-quench

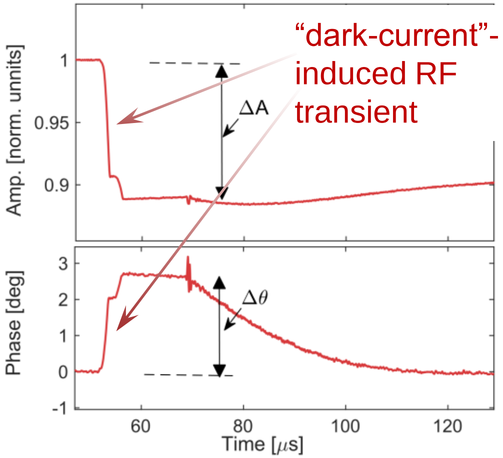

“dark-current”-induced transient (I/Q)

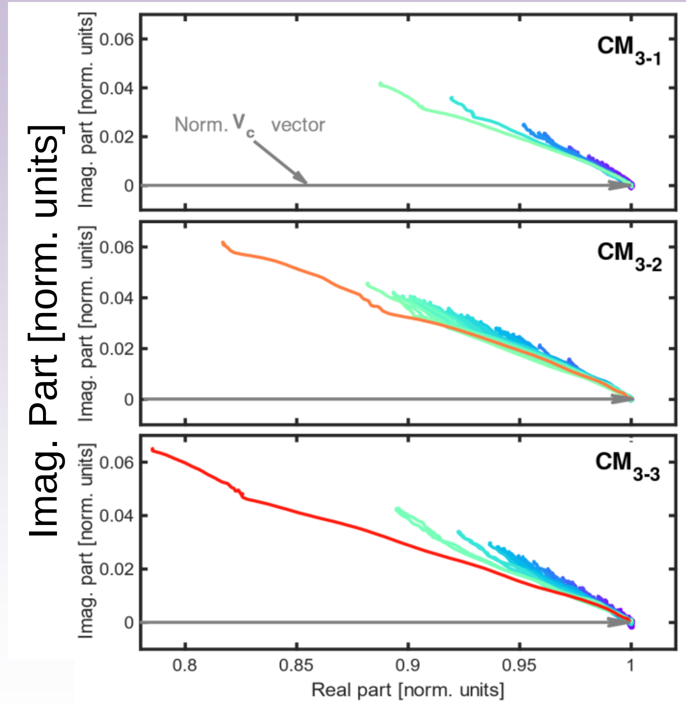

Statistical Distribution

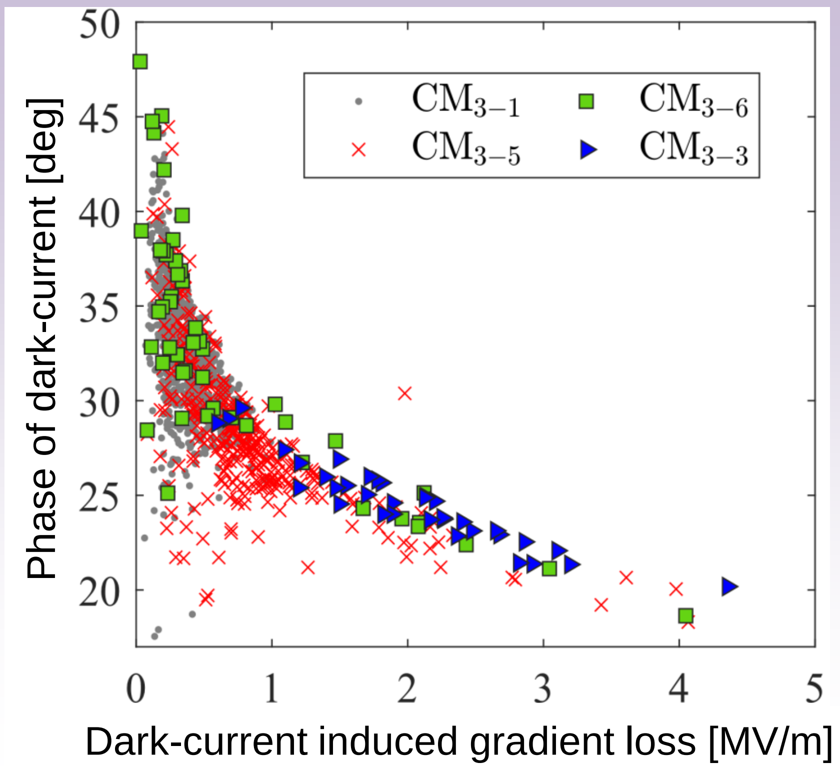

F. Qiu* et al., In-situ mitigation strategies of field emission induced cavity fault using low-level radio-frequency system, Nucl. Sci. Tech. 33:140, 2022

Mitigation of Burst-noise-induced SRF Faults (Results)

- Two types of **ponderomotive instabilities** are present in superconducting cavities: **monotonic** and **oscillatory** instabilities. In CAFe, oscillatory instability is the main issue.